

Diurnal and annual exchanges of mass and energy between an aspen-hazelnut forest and the atmosphere: Testing the mathematical model Ecosys with data from the BOREAS experiment

R. F. Grant,¹ T. A. Black,² G. den Hartog,³ J. A. Berry,⁴ H. H. Neumann,³ P. D. Blanken,² P. C. Yang,² C. Russell,⁵ and I. A. Nalder¹

Abstract. There is much uncertainty about the net carbon (C) exchange of boreal forest ecosystems, although this exchange may be an important part of global C dynamics. To resolve this uncertainty, net C exchange has been measured at several sites in the boreal forest of Canada as part of the Boreal Ecosystem-Atmosphere Study (BOREAS). One of these sites is the Southern Old Aspen site at which diurnal CO₂ and energy (radiation, latent, and sensible heat) fluxes were measured during 1994 using eddy correlation techniques at different positions within a mixed 70 year old aspen-hazelnut forest. These measurements were used to test a complex ecosystem model “ecosys” in which mass and energy exchanges between terrestrial ecosystems and the atmosphere are simulated hourly under diverse conditions of soil, management, and climate. These simulations explained between 70% and 80% of diurnal variation in ecosystem CO₂ and energy fluxes measured during three 1 week intervals in late April, early June, and mid-July. Total annual CO₂ fluxes indicated that during 1994, aspen was a net sink of 540 (modeled) versus 670 (measured) g C m⁻² yr⁻¹, while hazelnut plus soil were a net source of 472 (modeled) versus 540 (measured) g C m⁻² yr⁻¹. The aspen-hazelnut forest at the BOREAS site was therefore estimated to be a net sink of about 68 (modeled) versus 130 (measured) g C m⁻² yr⁻¹ during 1994. Long-term simulations indicated that this sink may be larger during cooler years and smaller during warmer years because C fixation in the model was less sensitive to temperature than respiration. These simulations also indicated that the magnitude of this sink declines with forest age because respiration increases with respect to fixation as standing phytomass grows. Confidence in the predictive capabilities of ecosystem models at decadal or centennial timescales is improved by well-constrained tests of these models at hourly timescales.

1. Introduction

Boreal forests are currently thought to be an important sink for atmospheric C [Keeling *et al.*, 1996]. However, the warming of these forests caused by rising CO₂ concentrations and temperatures hypothesized in some global climate change studies [e.g., Sellers *et al.*, 1996] have caused concern that this sink may be reduced, leading to increased C accumulation in the atmosphere. The sensitivity of net C exchange to climate change is determined by complex interactions between C fixation and respiration, each of which is in turn determined by complex responses to climate. Because net exchange is small in com-

parison to fixation and respiration [Black *et al.*, 1996], there is a need for accurate calculation of the responses of fixation and respiration to climate if reliable estimates of climate change effects on net C exchange are to be made. This need is most likely to be met by biophysically based ecosystem models that accurately represent the basic processes by which climate affects C fixation and respiration.

The sensitivity of net C exchange to hypothesized changes in climate will be primarily determined by the effects of rising CO₂ concentrations on mass and energy exchange between the forest canopies and the atmosphere, and by the effects of rising temperature on evapotranspiration and respiration by forest canopies and soils. The effects of CO₂ on mass and energy exchange arise from those on C fixation [Stitt, 1991] and stomatal conductance [Curtis, 1996]. The effect of CO₂ on C fixation is caused by its effect on rubisco specificity for CO₂ versus O₂ [Jordan and Ogren, 1984]. The magnitude of the CO₂ effect on C fixation is influenced by temperature [Idso *et al.*, 1987] through the effect of temperature on rubisco kinetics and on the solubility of CO₂ versus O₂. It is also influenced by irradiance [Allen *et al.*, 1990], because CO₂ affects light and dark reactions to differing degrees, and by nutrients [Kimball, 1993] through constraints that nutrient availability imposes upon rubisco kinetics. The effect of CO₂ on stomatal conductance occurs because CO₂ affects C fixation comparatively less

¹Department of Renewable Resources, University of Alberta, Edmonton, Canada.

²Department of Soil Science, University of British Columbia, Vancouver, Canada.

³Atmospheric Environment Service, Environment Canada, Downsview, Ontario.

⁴Department of Plant Biology, Carnegie Institution of Washington, Stanford, California.

⁵Department of Land Resource Science, University of Guelph, Guelph, Ontario, Canada.

Copyright 1999 by the American Geophysical Union.

Paper number 1998JD200117.

0148-0227/99/1998JD200117\$09.00

than it does CO_2 concentration gradients across stomata [Ball, 1988]. Changes in conductance with CO_2 cause CO_2 effects on C fixation to be influenced by plant water stress [Chaudhuri et al., 1990; Rogers et al., 1986]. The biological basis for each of these CO_2 effects on C fixation and stomatal conductance must be represented in ecosystem models used to study climate change effects on net C exchange.

Rising temperatures cause higher evapotranspiration by causing greater vapor pressure gradients to develop between the soil and plant surfaces and the atmosphere. Actual changes in evapotranspiration under hypothesized changes in climate will depend upon the extent to which higher evapotranspiration due to higher temperature will be offset by lower transpiration due to lower stomatal conductance under higher CO_2 . Sustained increases in temperature will eventually lead to lower soil and plant water status and hence lower stomatal conductance and C fixation. Rising temperatures also cause higher soil and plant respiration which if not offset by higher C fixation will cause net losses of soil C [Jenkinson et al., 1991; Kirschbaum, 1995; Parton et al., 1995]. The biological basis for each of these effects of temperature on evapotranspiration and respiration must be represented in ecosystem models used to study climate change effects on net C exchange.

Ecosystem models used to estimate climate change impacts on net C exchange should be based upon algorithms in which complex interactions among temperature, irradiance, nutrients, CO_2 and water on C, and water exchange are represented using basic biophysical principles. These interactions are highly dynamic and nonlinear, with pronounced temporal and spatial variation at a subdaily (e.g., hourly) timescale and at a subcanopy (e.g., leaf) spatial scale. Some of the current efforts [e.g., Bonan et al., 1997; Kimball et al., 1997; Frohling, 1997] to model these interactions use temporally aggregated climate data (irradiance, temperature, humidity, wind, and precipitation), usually at a daily timescale, and spatially aggregated vegetation, usually at a community scale, to calculate climatic effects on C and water exchange. However, the complex and nonlinear nature of climate interactions on C and water exchange may reduce confidence in the results of such aggregation. Results from these models cannot be tested directly against fluxes of mass and energy measured at subdaily timescales but rather against indices of these fluxes that have been aggregated to the same spatial and temporal scales as those at which the model functions. These indices (e.g., daily net C exchange) are the net results of several different interacting processes (e.g., transient plant C fixation and plant plus soil respiration), so model testing cannot be resolved to the process level at which it is better constrained.

We propose an alternative approach to the modeling of net C exchange in which the major processes of C transformation are first simulated and tested at temporal and spatial scales of the hour and the organ (e.g., leaf) or population (e.g., species). Results from these tests are then aggregated to and tested at temporal and spatial scales of the decade and the community [Grant, 1996a, b]. This approach benefits from the better constrained testing possible at higher temporal and spatial resolution while enabling the examination of model behavior at the lower temporal and spatial resolution at which ecosystem response to climate change must be evaluated.

Mass and energy exchange between the boreal forests and the atmosphere suitable for high-resolution model testing have been measured at several sites in the Boreal Ecosystem-Atmosphere Study (BOREAS) [Margolis and Ryan, 1997]. Ex-

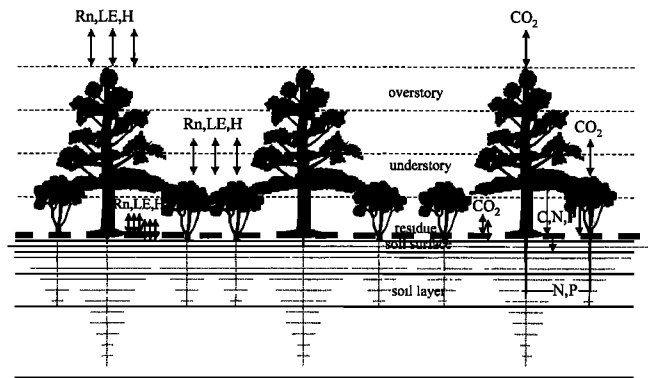


Figure 1. Mass and energy exchanges between the atmosphere and the complex soil and plant surfaces represented in “ecosys.” Rn, net radiation; LE, latent heat; H, sensible heat; C, carbon; N, nitrogen; P, phosphorus.

changes measured at the Southern Old Aspen site [Black et al., 1996] were selected for initial model testing because measurements were conducted at different spatial scales (organ, species, community) which allowed concurrent model testing. Measurements at other sites in BOREAS will be used for model testing at a later date.

2. Model Development

2.1. Ecosystem-Atmosphere Energy Exchange

The accurate simulation of energy exchange between the atmosphere and the terrestrial surfaces is a key requirement of ecosystem models such as “ecosys,” because this exchange is believed to affect the exchange and transport of energy in the atmosphere and hence to affect climate. Ecosystem-atmosphere energy exchange is strongly controlled by ecosystem water and nutrient status, so that these controls must be accurately represented in ecosystem models.

Energy exchange between the atmosphere and the terrestrial surfaces is resolved hourly in ecosys into that between the atmosphere and the canopy of each plant species, as described by Grant et al. [1998, equations (1)–(15)] and elsewhere [Grant and Baldocchi, 1992; Grant et al., 1993e, 1995c] and that between the atmosphere and each of snow, residue, and soil surfaces [Grant et al., 1998, equations (16)–(23)], Grant [1992], Grant et al. [1995b] (Figure 1). Total energy exchange between the atmosphere and the terrestrial surfaces is calculated as the sum of the exchanges with each plant canopy and each snow, residue, and soil surface.

Canopy energy exchange in ecosys is calculated from an hourly two-stage convergence solution for the transfer of water and heat through a multispecific, multilayered soil-root-canopy system. The first stage of this solution requires convergence to a canopy temperature at which the first-order closure of the energy balance is achieved for the canopy of each plant species. The energy balance requires first that the absorption, reflection and transmission of both shortwave and photosynthetically active radiation be calculated for each leaf and stem surface in a multilayered canopy. Radiation includes direct and diffuse sources, defined by solar and sky angles as well as forward and backscattering within the canopies. Leaf and stem surfaces are defined by species, height, azimuth, inclination, exposure (sunlit versus shaded) and optical properties. Nonuniformity in the

horizontal distribution of leaf surfaces within each canopy layer (clumping) is represented by a species-specific interception fraction between zero and 1 which describes the fractional exposure of leaf and stem surfaces to direct and diffuse irradiance (versus self-shading). The fraction of photosynthetic photon flux density absorbed by each canopy is used to partition the exchange of longwave radiation emitted by sky, ground, and canopy surfaces, the net values of which are added to total shortwave radiation absorbed by all leaf and stem surfaces to calculate canopy net radiation.

The energy balance then requires solutions for latent and sensible heat fluxes at the temperature of each canopy. If free water is present on leaf or stem surfaces, latent heat flux is calculated from evaporation determined by canopy-atmosphere vapor density gradient and aerodynamic conductance. If free water is not present, latent heat flux is calculated from transpiration from leaf surfaces, which is also determined by stomatal conductance. Sensible heat flux is calculated from canopy-atmosphere temperature gradient and aerodynamic conductance. Canopy heat storage is calculated from changes in canopy temperature and from the masses and water contents of leaves, twigs, and stems.

Aerodynamic conductance in energy balance solutions is calculated from zero plane displacement and surface roughness heights of each canopy derived from their heights and leaf areas [Perrier, 1982]. Aerodynamic conductance of nondominant canopies is reduced according to the differences between their heights and that of the dominant canopy, as proposed by Choudhury and Monteith [1988]. Stomatal conductance is calculated for each leaf surface of each canopy from leaf carboxylation rate and from the CO₂ concentration gradient across its stomates [Grant et al., 1998, equations (48)–(53)]. Leaf conductances are aggregated to the canopy level for energy balance calculations [Grant et al., 1998, equations (13)–(15)]. Two controlling mechanisms are postulated for stomatal conductance: (1) leaf carboxylation rate at nonlimiting water potential as determined by ambient irradiance, temperature, and CO₂, and (2) canopy turgor potential at ambient total and osmotic water potentials [Grant et al., 1998, equations (24) and (25)] as determined by canopy water potential. The calculation of leaf carboxylation rate and canopy turgor potential is described below. A hypothesis that stomatal conductance is controlled by root-derived signals [e.g., Gollan et al., 1986] is not yet included in the model because of uncertainty in its parameterization.

2.2. Canopy Water Relations

The simulation of water status effects on energy exchange is based on coupling the uptake of water from the soil through the root to the canopy with the evaporation of water from the canopy to the atmosphere. This coupling determines the water status of the canopy and hence its conductance to water vapor.

The second stage of the hourly solution for heat and water transfer therefore requires convergence to a water potential for each canopy at which the difference between canopy transpiration and root water uptake [Grant et al., 1998, equations (32)–(37)] equals the difference between canopy water content at its previous water potential and that at its current water potential. Canopy water potential controls transpiration by determining canopy turgor (calculated as the difference between canopy water and osmotic potentials) which affects stomatal conductance and thereby canopy temperature, vapor pressure, and conductance to vapor transfer. Canopy water potential controls root water uptake by determining canopy-

soil water potential gradients, which are also determined by soil-root and root-canopy hydraulic conductances in each rooted soil layer. Soil-root conductance is calculated from root length, given by a root growth submodel [Grant, 1993a, b, 1998a; Grant and Robertson, 1997], and from soil-root hydraulic conductivity calculated according to Cowan [1965]. Root-canopy conductance is calculated from radial and axial conductances [Reid and Huck, 1990] of primary and secondary roots, as described by Grant [1998a]. If the convergence criterion for difference between canopy transpiration and uptake versus change in canopy water content is not met, the energy balance is solved again using an adjusted value for canopy water potential. The convergence is then repeated using new values for transpiration, uptake, and change in canopy water content calculated from the adjusted water potential.

2.3. Canopy C Fixation

Because leaf C fixation rate partly determines leaf conductance to water vapor, the accurate simulation of leaf C fixation is an important requirement of ecosystem models. Leaf C fixation is determined by carboxylation, which is controlled by irradiance, temperature, and leaf CO₂ concentration, and by diffusion, which is controlled by the atmosphere-leaf CO₂ concentration gradient and leaf conductance. The coupling of carboxylation and diffusion in ecosys allows the calculation of a leaf C fixation rate, which is then aggregated to the canopy level.

This coupling occurs after successful completion of the second stage of the convergence solution for heat and water transfer, when a convergence solution [Grant et al., 1998, equation (54)] is used to calculate gaseous CO₂ concentration and its aqueous equivalent in the mesophyll of each leaf surface in each canopy. These are the concentrations at which the diffusion rate of gaseous CO₂ [Grant et al., 1998, equation (48)] equals the carboxylation rate of aqueous CO₂ within each leaf surface [Grant et al., 1998, equation (47)]. The diffusion rate is calculated from the concentration gradient across the stomates divided by the stomatal conductance [Grant et al., 1998, equations (49) and (50)] given from the convergence solution for heat and water transfer described above. The carboxylation rate is the minimum of that from dark and light reactions [Grant et al., 1998, equations (38)–(46)] calculated according to Farquhar et al. [1980]. These reactions are driven by the product of the specific activities and areal concentrations of rubisco or chlorophyll at each node. These concentrations are determined by the growth of each leaf as affected by environmental conditions (CO₂, radiation, temperature, water, nitrogen). The photosynthetic photon flux density by which the light-limited carboxylation rate is controlled is given by the absorption of photosynthetically active radiation described above. The CO₂ fixation rate of each leaf surface is added to arrive at a value for gross CO₂ fixation by each branch of each canopy.

2.4. Canopy C Respiration

Plants both fix and respire C, so net C exchange between plants and the atmosphere is the difference between the two. If ecosystem models are used to calculate net C exchange and hence ecosystem contributions to atmospheric CO₂ concentrations, the accurate simulation of C respiration is essential. Respiration has two components: maintenance respiration, required to maintain the biological integrity of the plant, and growth respiration, required to form new plant material.

The hourly product of CO₂ fixation is added to a C storage

pool for each branch of each canopy from which C is oxidized hourly to meet maintenance and growth respiration requirements [Grant *et al.*, 1998, equations (27) and (28)]. Low C storage may cause C oxidation to be less than maintenance respiration, in which case the difference is made up through respiration of remobilizable C (considered to be equal to the protein fraction) of leaf and twig C. Remobilization starts at the lowest node at which leaves and twigs are present and proceeds upward. Upon exhaustion of the remobilizable C in each leaf or twig, the remaining C is dropped from the branch and added to the soil surface. Environmental constraints such as N, heat, or water stress which reduce C fixation with respect to maintenance respiration will therefore accelerate the loss of leaf and twig C from the plant. Net CO₂ fixation is calculated for each branch as the difference between gross fixation and the sum of maintenance, growth, and senescence respiration.

2.5. Nutrient Uptake

The simulation of nutrient status effects on energy exchange is based on the coupling of nutrient (nitrogen N and phosphorus P) uptake from the soil through the root to the canopy with nutrient assimilation in the root and canopy. This coupling determines nutrient concentrations in the leaf which in turn determine leaf carboxylation rates and hence leaf conductance.

Nutrient (N and P) uptake is calculated hourly for each plant species by iteratively converging toward values for aqueous concentrations at its root and mycorrhizal surfaces in each soil layer at which radial transport by mass flow and diffusion from the soil solution to the surfaces equals active uptake by the surfaces [Grant and Robertson, 1997, equation (14)]. The aqueous concentrations of nutrients in each soil layer are controlled by precipitation, adsorption, and ion-pairing reactions [Grant and Heaney, 1997], solute transport [Grant and Heaney, 1997], and microbial activity [Grant *et al.*, 1993a, b]. Mass flow is calculated from root water uptake described above, and diffusion is calculated from root length densities given by the root growth submodel [Grant, 1993a, b, 1998a; Grant and Robertson, 1997]. Root uptake is calculated from root surface area [Itoh and Barber, 1983], given by the root growth submodel, and is constrained by root oxygen uptake and nutrient storage [Grant, 1998a].

2.6. Plant Growth

Growth respiration drives expansive growth of vegetative and reproductive organs at different nodes of each shoot branch through mobilization of storage C, N, and P according to phenology-dependent partitioning coefficients and biochemically based growth yields [Grant and Hesketh, 1992]. This growth is used to calculate the lengths, areas, and volumes of individual internodes, sheaths, and leaves [Grant, 1994a; Grant and Hesketh, 1992] from which heights and areas of leaf and stem surfaces are calculated for irradiance interception and aerodynamic conductance algorithms described above. Growth respiration also drives extension of primary and secondary root axes and of mycorrhizal axes of each plant species in each soil layer through mobilization of storage C, N, and P as described by Grant [1993a]. This growth is used to calculate lengths and areas of root and mycorrhizal axes from which root uptake of water [Grant *et al.*, 1998] and nutrients [Grant and Robertson, 1997] is calculated. Transfers of storage C, N, and P among different shoot branches and root axes are driven by concentration gradients [Grant, 1998a] which arise from the proximity of each plant part to the site of resource acquisition and from

the resource consumption rate of each plant part. Storage N or P concentration and turgor potential may constrain C oxidation for growth in different parts of the shoot and root, causing storage C to migrate toward zones of lower C concentration where C oxidation is more rapid. Low storage N or P concentrations may also reduce leaf N and P concentrations, thereby reducing leaf carboxylation rates and hence leaf conductance. For perennial plant species, soluble C, N, and P are withdrawn from storage pools in shoot branches into a long-term storage pool in the crown during autumn, causing leaf senescence. Soluble C, N, and P are remobilized from this pool to drive leaf and twig growth the following spring. The timing of withdrawal and remobilization is determined by duration of exposure to cool temperatures (between 3° and 8°C) under shortening and lengthening photoperiods, respectively.

2.7. Soil Microbial Activity

The aqueous concentrations at which nutrients are maintained in the soil and hence the rates at which they are taken up by plants are strongly controlled by microbial activity in the soil. This activity is coupled to the oxidation of soil C and the reduction of O₂ and other electron acceptors and hence to the exchange of C with the atmosphere. The accurate simulation of soil microbial activity is therefore an important requirement of ecosystem models.

Microbial activity in ecosystems is represented as a parallel set of substrate-microbe complexes [Grant *et al.*, 1993a, b] which include the rhizosphere [Grant, 1993c], plant residues and animal manure [Grant and Rochette, 1994], and native organic matter [Grant *et al.*, 1993a, b]. Within each complex the activities of obligately aerobic, facultatively anaerobic, and obligately anaerobic heterotrophs are simulated hourly at the temperatures and water contents of plant surface residue and of a spatially resolved soil profile [Grant, 1997; Grant and Rochette, 1994; Grant *et al.*, 1997] given from the energy balance calculations described above. Aspen and hazelnut residues are partitioned into carbohydrate, protein, cellulose, and lignin fractions according to Trofymow *et al.* [1995], each of which is of differing vulnerability to hydrolysis by heterotrophic decomposers (Table 3). Soil organic matter is also partitioned into fractions of differing vulnerability to hydrolysis. All heterotrophic populations conduct C oxidation to support growth and maintenance processes, the total of which drives CO₂ emission from the soil surface. This oxidation is coupled to the reduction of O₂ by all aerobic populations (including populations of N₂ fixers), to the sequential reduction of NO₃⁻, NO₂⁻, and N₂O by heterotrophic denitrifiers [Grant *et al.*, 1993c, d; Grant and Pattey, 1999] and to the reduction of acetate by heterotrophic methanogens [Grant, 1998b]. In addition, autotrophic nitrifiers conduct NH₄⁺ and NO₂⁻ oxidation [Grant, 1994b] and N₂O evolution [Grant, 1995], and autotrophic methanotrophs conduct CH₄ oxidation [Grant, 1999].

The rates of all heterotrophic and autotrophic oxidations are driven by changes in the free energies of reactants and products. All soluble and gaseous reactants and products undergo convective-dispersive transport through the soil profile [Grant *et al.*, 1993c; Grant and Heaney, 1997].

3. Field Experiment

3.1. Site Description

The Southern Old Aspen site of BOREAS is located at 53.7°N 106.2°W (Prince Albert National Park, Saskatchewan,

Table 1. Physical and Biological Properties of the Orthic Gray Luvisol at the Southern Old Aspen Site Reported by D. Anderson (TE-01) and used in "Ecosys"

| | Depth, m | | | | | | | | | | |
|---|----------|-------|-------|-------|-------|-------|-------|-------|-------|-------|-------|
| | 0.01 | 0.03 | 0.06 | 0.16 | 0.45 | 0.61 | 0.81 | 1.01 | 1.43 | 1.79 | 1.95 |
| BD, Mg m ⁻³ | 0.16 | 0.16 | 0.16 | 1.24 | 1.53 | 1.53 | 1.53 | 1.42 | 1.53 | 1.53 | 1.53 |
| $\theta_{-0.03\text{MPa}}$, m ³ m ⁻³ | 0.40 | 0.40 | 0.40 | 0.149 | 0.211 | 0.196 | 0.175 | 0.194 | 0.177 | 0.245 | 0.257 |
| $\theta_{-1.5\text{MPa}}$, m ³ m ⁻³ | 0.20 | 0.20 | 0.20 | 0.061 | 0.130 | 0.113 | 0.106 | 0.125 | 0.089 | 0.138 | 0.157 |
| Sand, kg kg ⁻¹ | 0.0 | 0.0 | 0.0 | 610 | 484 | 576 | 514 | 486 | 484 | 550 | 364 |
| Silt, kg kg ⁻¹ | 0.0 | 0.0 | 0.0 | 281 | 222 | 190 | 263 | 281 | 276 | 312 | 396 |
| pH | 6.7 | 6.7 | 6.8 | 6.4 | 6.5 | 6.6 | 8.2 | 8.3 | 8.4 | 8.5 | 8.9 |
| CEC, cmol kg ⁻¹ | 110 | 110 | 67.0 | 8.2 | 19.1 | 15.0 | 11.6 | 11.4 | 8.3 | 11.7 | 13.3 |
| Org. C, g kg ⁻¹ | 397 | 397 | 331 | 6.5 | 5.1 | 3.0 | 4.2 | 4.0 | 3.5 | 3.6 | 4.6 |
| Org. N, mg kg ⁻¹ | 21246 | 21246 | 20596 | 483 | 491 | 351 | 289 | 280 | 257 | 249 | 195 |
| Org. P, mg kg ⁻¹ | 1741 | 1741 | 1379 | 216 | 237 | 324 | 494 | 454 | 505 | 529 | 511 |

Org, organic.

Canada) near the southern limit of the boreal forest on an Orthic Gray Luvisol (Typic Haploboroll, Table 1) overlying a glacial till. The overstory at this site is 70 year old aspen (*Populus tremuloides* Michx.), 21.5 m high with a stem density of 860 ha⁻¹. The understory is dominated by hazelnut (*Corylus cornuta* Marsh.), 2 m high with occasional wild rose (*Rosa woodsii* Lindl.) and alder (*Alnus crispa* Pursh).

3.2. Canopy Mass and Energy Exchange

Fluxes were measured during 1994 using eddy correlation with sonic anemometers mounted above the aspen overstory at 39 m (DAT-310, Kaijo-Denki, Tokyo) and above the hazelnut understory at 4 m (model 1012R2A Solent, Gill Instruments, Lymington, England) and with closed-path infrared gas analyzers (model 6262, LI-COR Inc., Lincoln, Nebraska). Instantaneous measurements of vertical wind speed and scalar quantities at 20 Hz were used to calculate half-hourly average fluxes with corrections for air density and sample cell pressure. Vapor densities measured at 4 m were checked against those from an open-path H₂O analyzer (model K20 hygrometer, Campbell Scientific, Logan, Utah). Net radiation was measured with net radiometers mounted on the main flux tower at 33 m (model S-1, Swissteco Instruments, Oberriet, Switzerland) and on a 65 m mobile tram at 4 m (models S-1 and S-14 miniature, Swissteco Instruments).

Daytime CO₂ flux was measured during 1994 at the soil surface with a soil respiration chamber (model 6000-09 LI-COR) attached to PVC collars and a portable photosynthesis system (model 6200 LI-COR). Meteorological data, including global shortwave radiation, air temperature, wind speed, humidity and precipitation, were recorded as 15 min averages during 1994, 1995, and 1996 over the aspen canopy at the Southern Old Aspen site, as described by *Shewchuk* [1996]. Yearly-averaged climate data are given in Table 2. Further details about site measurements are reported by *Blanken et al.* [1997] and *Black et al.* [1996].

Table 2. Yearly Averaged Climate Data Recorded at the Southern Old Aspen Site During 1994, 1995, and 1996

| | 1994 | 1995 | 1996 |
|---|-------|-------|-------|
| Maximum temperature, °C | 6.16 | 4.83 | 3.73 |
| Minimum temperature, °C | -2.96 | -3.49 | -5.01 |
| Solar radiation, MJ m ⁻² d ⁻¹ | 11.03 | 11.45 | 11.10 |
| Precipitation, mm d ⁻¹ | 1.17 | 1.08 | 1.14 |

3.3. Leaf CO₂ Fixation

On August 24, 1994, selected leaves near the tops of the aspen and hazelnut canopies were enclosed in the cuvette of a portable gas exchange system (model MPH-1000, Campbell Scientific, Logan, Utah) with an infrared gas analyzer (model 6262, LiCor Inc., Lincoln, Nebraska) and a dew point mirror (model Dew-10, General Eastern, Woburn, Massachusetts) which enabled precise control of CO₂, temperature, irradiance, and humidity at the leaf surface. The leaves were subjected to incremental changes in either CO₂ concentration, air temperature, or irradiance with all other environmental conditions held constant. Response of CO₂ flux to CO₂ concentration was measured at high irradiance (about 1000 μmol m⁻² s⁻¹) and high chamber humidity (70–80%). Response of CO₂ flux to irradiance was measured after preconditioning to 1000 μmol m⁻² s⁻¹. Irradiance was then increased in steps of about 300 μmol m⁻² s⁻¹ until saturation was evident and then decreased in steps to zero. Response of CO₂ flux to temperature was measured by increasing chamber temperature from 15° to 35°C in steps of 2.5°C under saturating irradiance and constant dew point temperature. This protocol was chosen to mimic the covariation of leaf temperature and vapor pressure deficit that occurs naturally on warm, dry days in this environment. Measurements of CO₂ flux and stomatal conductance were taken when steady state values were achieved (usually 30 min after conditions were changed).

3.4. Ecosystem C Distribution

Allometric equations relating diameter measured at 1.4 m above ground to biomass of stem, branch, and foliage, to sapwood volume, and to leaf area were developed by *Gower et al.* [1997] for each tree within each of four 30 m × 30 m replicated plots near the flux tower at the Southern Old Aspen site. Each of these trees was taken to represent a number of other trees of similar stature on an areal basis in order to scale all measurements from the plot to the hectare. Understory vegetation was removed from a 2 m × 2 m subplot randomly located in each of the 30 m × 30 m main plots and stored at 3°C. Samples of this vegetation were separated into ephemeral plant material, and into new or old foliage and twigs from perennial plants. Sample components were then dried and weighed.

Distances between adjacent rings were measured by *Gower et al.* [1997] to the nearest μm (Dual Axis Optical Micrometer and Spalding B5 Digital Position Display System, Gaertner Scientific, Chicago, Illinois) in cores removed from each tree in

Table 3. Biological Properties of Aspen, Hazelnut, and Soil Microbial Populations Used in Ecosys

| Variable | Value | Units |
|---|--------|---|
| <i>Aspen and Hazelnut</i> | | |
| Maximum carboxylation rate | 50 | $\mu\text{mol CO}_2 \text{ g}^{-1} \text{ rubisco s}^{-1}$ |
| Maximum rubisco oxygenation rate | 10.5 | $\mu\text{mol O}_2 \text{ g}^{-1} \text{ rubisco s}^{-1}$ |
| Maximum electron transport rate | 500 | $\mu\text{mol e}^- \text{ g}^{-1} \text{ chlorophyll s}^{-1}$ |
| Quantum efficiency | 0.5 | $\mu\text{mol e}^- \mu\text{mol quanta}^{-1}$ |
| M-M constant for carboxylation | 12.5 | $\mu\text{M CO}_2$ |
| M-M constant for oxygenation | 500 | $\mu\text{M O}_2$ |
| Fraction of leaf protein in rubisco | 0.25 | $\text{g C g}^{-1} \text{ C}$ |
| Fraction of leaf protein in chlorophyll | 0.05 | $\text{g C g}^{-1} \text{ C}$ |
| Maximum N:C ratio in leaf | 0.15 | $\text{g N g}^{-1} \text{ C}$ |
| N:C ratio in twig and root | 0.0375 | $\text{g N g}^{-1} \text{ C}$ |
| N:C ratio in stem | 0.0025 | $\text{g N g}^{-1} \text{ C}$ |
| Maintenance respiration of plant | 0.016 | $\text{g C g}^{-1} \text{ N h}^{-1} \text{ at } 30^\circ\text{C}$ |
| Growth yield of leaf and twig | 0.64 | $\text{g C g}^{-1} \text{ C}$ |
| Growth yield of stem | 0.84 | $\text{g C g}^{-1} \text{ C}$ |
| Growth yield of root | 0.64 | $\text{g C g}^{-1} \text{ C}$ |
| Interception fraction, aspen | 0.65 | $\text{m}^2 \text{ m}^{-2}$ |
| Interception fraction, hazelnut | 1.0 | $\text{m}^2 \text{ m}^{-2}$ |
| <i>Soil</i> | | |
| Decomposition of residue carbohydrate | 1.0 | $\text{g res. C g}^{-1} \text{ micr. C h}^{-1}$ |
| Decomposition of residue protein | 1.0 | $\text{g res. C g}^{-1} \text{ micr. C h}^{-1}$ |
| Decomposition of residue cellulose | 0.15 | $\text{g res. C g}^{-1} \text{ micr. C h}^{-1}$ |
| Decomposition of residue lignin | 0.025 | $\text{g res. C g}^{-1} \text{ micr. C h}^{-1}$ |
| Decomposition of soil particulate matter | 0.025 | $\text{g res. C g}^{-1} \text{ micr. C h}^{-1}$ |
| Decomposition of soil humus | 0.005 | $\text{g res. C g}^{-1} \text{ micr. C h}^{-1}$ |
| Microbial specific respiration rate | 0.20 | $\text{g C g}^{-1} \text{ micr. C h}^{-1} \text{ at } 30^\circ\text{C}$ |
| M-M const. for microbial C uptake | 35 | g C m^{-3} |
| Maintenance respiration of labile microbe | 0.010 | $\text{g C g}^{-1} \text{ N h}^{-1} \text{ at } 30^\circ\text{C}$ |
| Maintenance respiration of resistant microbe | 0.0015 | $\text{g C g}^{-1} \text{ N h}^{-1} \text{ at } 30^\circ\text{C}$ |
| Microbial growth yield on O ₂ | 0.60 | $\text{g C g}^{-1} \text{ C}$ |
| Microbial growth yield on NO _x | 0.25 | $\text{g C g}^{-1} \text{ C}$ |
| Microbial N ₂ fixation yield on O ₂ | 0.16 | $\text{g N g}^{-1} \text{ C}$ |

the sample plots. Annual increments in tree diameters calculated from these differences were used with the allometric equations described above to estimate overstory growth. Litterfall was collected each fall and spring from $1 \times 1 \text{ m}$ screens in each plot and separated into leaf and nonleaf components. The leaf component was further separated by species. This work is described further by Gower *et al.* [1997].

Ten soil cores (10 cm diameter \times 30 cm depth) were taken by Steele *et al.* [1997] from each plot on April 28–30, 1994, before soil thawing was complete. The soil was separated by horizon, composited by plot, mixed, and sieved to pass through a 1 cm mesh screen. As many fine roots as possible were removed, after which the root-free soil was returned by horizon into each hole and the forest floor was replaced on top. In June 1995 and 1996, five cores per plot were removed with a corer (5 cm diameter \times 30 cm depth), stored in plastic bags at 3°C , and then elutriated (Gillison's Variety Fabrication Inc., Benzonia, Michigan). Roots recovered from the elutriation were sorted and classified as herbaceous or woody, dried at 70°C , and weighed. Fine root growth was calculated from changes in fine root mass over time by Steele *et al.* [1997].

Allometric equations relating diameter measured at 1.4 m above ground to aspen wood biomass were used to estimate wood biomass of differently aged aspen stands (as measured from ^{14}C dating of subsurface ash layers) at several other sites in Prince Albert National Park where the Southern Old Aspen site is located.

4. Model Experiment

4.1. Model Initialization and Run

The ecosystem model ecosys was initialized with data for the physical properties of the Orthic Gray Luvisol at the Southern Old Aspen site [Anderson, 1995, Table 1], and with parameters for the biological properties of aspen and hazelnut (assumed to be identical), and of soil microbial populations (Table 3). All model parameters for C fixation and respiration by plant and microbial populations were the same as those used in earlier studies of C and energy exchange over agricultural crops [Grant and Baldocchi, 1992; Grant *et al.*, 1993e, 1995c, 1999c] and soils [Grant, 1994a, 1997; Grant and Rochette, 1994; Grant *et al.*, 1993a, b, c, d, 1995b, 1997]. Model parameters for plant architecture and growth habit were those of a perennial deciduous tree. No alteration of model parameters from those used in earlier studies was conducted for the aspen-hazelnut study reported here.

The model was then run for 100 years under random yearly sequences of hourly-averaged meteorological data recorded in 1994, 1995, and 1996. During the first year of the run, aspen and hazelnut were seeded onto bare soil at 0.1 and 1.0 m^{-2} , respectively. The aspen was provided with a small C reserve to simulate regrowth from C stored in roots. At the beginning of every tenth year of the model run, all hazelnut stems were transferred from standing phytomass to surface residue, so new stems regrew from the soil surface the following spring.

4.2. Model Results

During the seventieth year of the model run, hourly mass and energy exchange over aspen and hazelnut simulated with 1994 meteorological data were compared with results obtained from the overstory and understory flux towers at the field site during 1994. Simulated CO₂ and energy fluxes over the aspen were calculated as the sum of those from the soil surface, the surface residue, the hazelnut, and the aspen. Simulated CO₂ and energy fluxes over the hazelnut were calculated as the sum of those from the soil surface, the surface residue, and the hazelnut. Three 1 week periods were selected for comparison. The first was in early spring (April 24 to May 1) after snowmelt and before leaf-out to observe model behavior when foliage was not present. The second was in late spring (June 7–14) during a transition from clear to cloudy weather to observe model response to changing atmospheric conditions. The third was in midsummer (July 15–22) when radiation and temperature were greatest to observe model simulation of larger mass and energy fluxes.

After completion of the model run, all state variables in the model were initialized with the values they had held at the end of August 23 of the year during which the mass and energy exchange comparisons described above were made. The model was then run for 24 hours during which incremental changes were made in either atmospheric CO₂ concentration, air temperature, or irradiance with all other environmental conditions held constant at values used in the leaf CO₂ fixation study described above. CO₂ fixation rates and stomatal conductances simulated for an individual leaf surface in the upper part of both the aspen and the hazelnut canopies were compared with measured values.

Model results for annual net primary productivity (NPP), net ecosystem exchange (NEE), and aboveground phytomass growth of a 70 year old aspen-hazelnut forest under 1994 climate were then compared with estimates of NPP, NEE, and growth derived from aggregated flux data and from tree ring analysis during 1994. Model results for C accumulation in different ecosystem components (e.g., leaves, roots, forest floor) were also compared with data obtained from the field site and from other related sites. Long-term model results for C accumulation in aspen stems and branches were compared with results of allometric studies of aspen growth in the same ecological zone as that of the field site.

5. Results

5.1. Leaf CO₂ Fixation and Stomatal Conductance

The responses of CO₂ fixation and stomatal conductance by selected leaf surfaces to increasing temperature, irradiance, and CO₂ concentration simulated on August 24 of the seventieth year of the model run are compared in Figure 2 with responses measured at the Southern Old Aspen site on August 24, 1994. In the model these responses were greater for aspen than for hazelnut because aspen leaves had lower specific leaf areas and hence higher areal N concentrations and thereby rubisco densities. Leaf N concentrations simulated under the soil and climatic conditions of the field site declined from ~0.09 g N g C⁻¹ in early spring to ~0.07 g N g C⁻¹ during late summer, which is consistent with average values of 0.08 g N g C⁻¹ reported from the Northern Old Aspen site by *Dang et al.* [1997]. The responses of CO₂ fixation and stomatal conductance to increasing temperature in the model arise from com-

plex interactions among several processes. These include changing CO₂/O₂ concentrations caused by declining gaseous solubilities, changing carboxylation, oxygenation and electron transport rates caused by more rapid reaction kinetics, and declining turgor potentials caused by increasing vapor pressure differences. These interactions caused simulated leaf CO₂ fixation and stomatal conductance to increase with temperature below 20°C, and to decrease with temperature above 20°C for the conditions of irradiance, CO₂, and vapor pressure under which the field measurements were taken (Figures 2a, 2b). In the model, increases at lower temperatures were attributed to more rapid reaction kinetics, while declines at higher temperatures were attributed to lower CO₂:O₂ ratios and to lower turgor potentials. These lower potentials were calculated from the convergence solution described above for equilibrating soil-root-canopy water uptake with canopy-atmosphere vapor diffusion under canopy-atmosphere vapor pressure gradients that rose with temperature. *Hogg and Hurdle* [1997] reported that stomatal conductance of aspen at the field site declined when vapor pressure gradients exceeded 1 kPa, a value reached at 18°C in this study. The simulated response of leaf CO₂ fixation to increasing temperature was more pronounced than that measured (Figure 2a) and that of stomatal conductance did not reproduce the higher values measured below 20°C (Figure 2b).

The responses of leaf CO₂ fixation and stomatal conductance to increasing irradiance in the model are determined by the interaction between light and dark reactions on CO₂ fixation under ambient temperature, CO₂, and vapor pressure. The initial slope of the irradiance response curves of aspen and hazelnut were the same (Figure 2c), suggesting that the common value of quantum efficiency used in the model (Table 3) for irradiance-limited CO₂ fixation was accurate. The transition to irradiance-saturated CO₂ fixation occurred at higher irradiance for aspen than for hazelnut, due in the model to higher areal rubisco density and hence higher maximum dark reaction rates in the aspen. Stomatal conductance rose with CO₂ fixation under increasing irradiance (Figure 2d) as required in the model to maintain a constant CO₂ concentration ratio across the stomates.

The responses of leaf CO₂ fixation and stomatal conductance to increasing CO₂ concentration in the model are determined by the Michaelis-Menten constants for carboxylation and oxygenation (Table 3) and by the effects of CO₂ on the compensation point and thereby on the carboxylation efficiencies of the light and dark reactions. Leaf CO₂ fixation rose hyperbolically with CO₂ concentration under the irradiance, temperature, and vapor pressure of the field study (Figure 2e), forcing stomatal conductance to decline (Figure 2f) in order to maintain a constant CO₂ concentration ratio across the stomates in the model.

5.2. Canopy Mass and Energy Exchange

5.2.1. Early spring. During the April comparison period, solar radiation and air temperature were rising (Figure 3a), while vapor concentration and precipitation remained low (average daytime RH ≈ 50%) (Figure 3b). Snowmelt was mostly complete by DOY 100 (April 10) in the model and DOY 102 (April 12) in the field. In the absence of leaf surfaces, most radiant energy received by the aspen-hazelnut forest during the week was returned to the atmosphere as sensible heat over both the aspen (Figure 4a) and the hazelnut (Figure 4b) (simulated versus measured sensible heat fluxes: over aspen, $R^2 =$

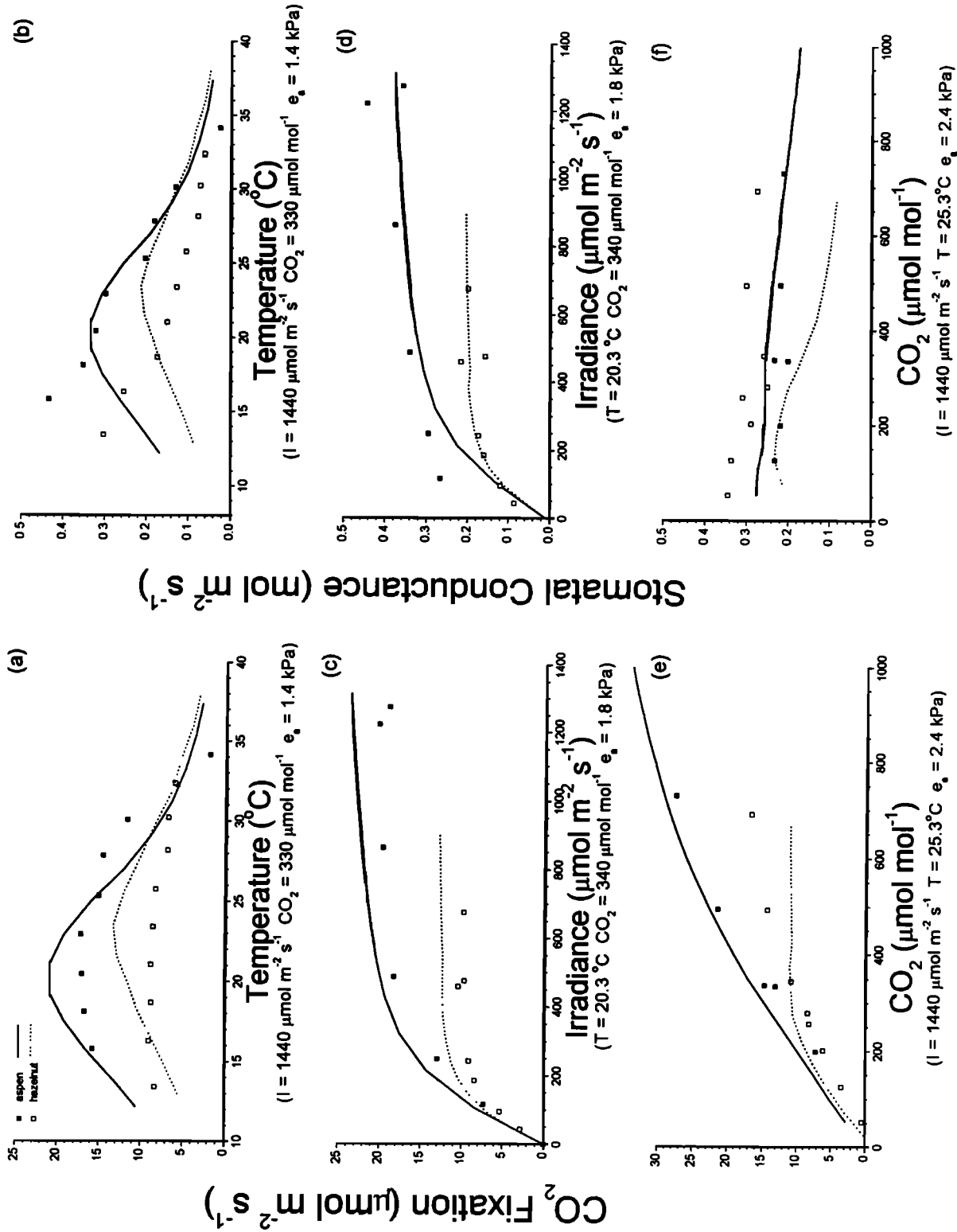


Figure 2. Simulated (lines) and measured (symbols) responses of CO_2 fixation and stomatal conductance by a horizontal leaf surface in the upper part of aspen and hazelnut canopies to changes in (a, b) air temperature, (c, d) irradiance, and (e, f) atmospheric CO_2 concentration.

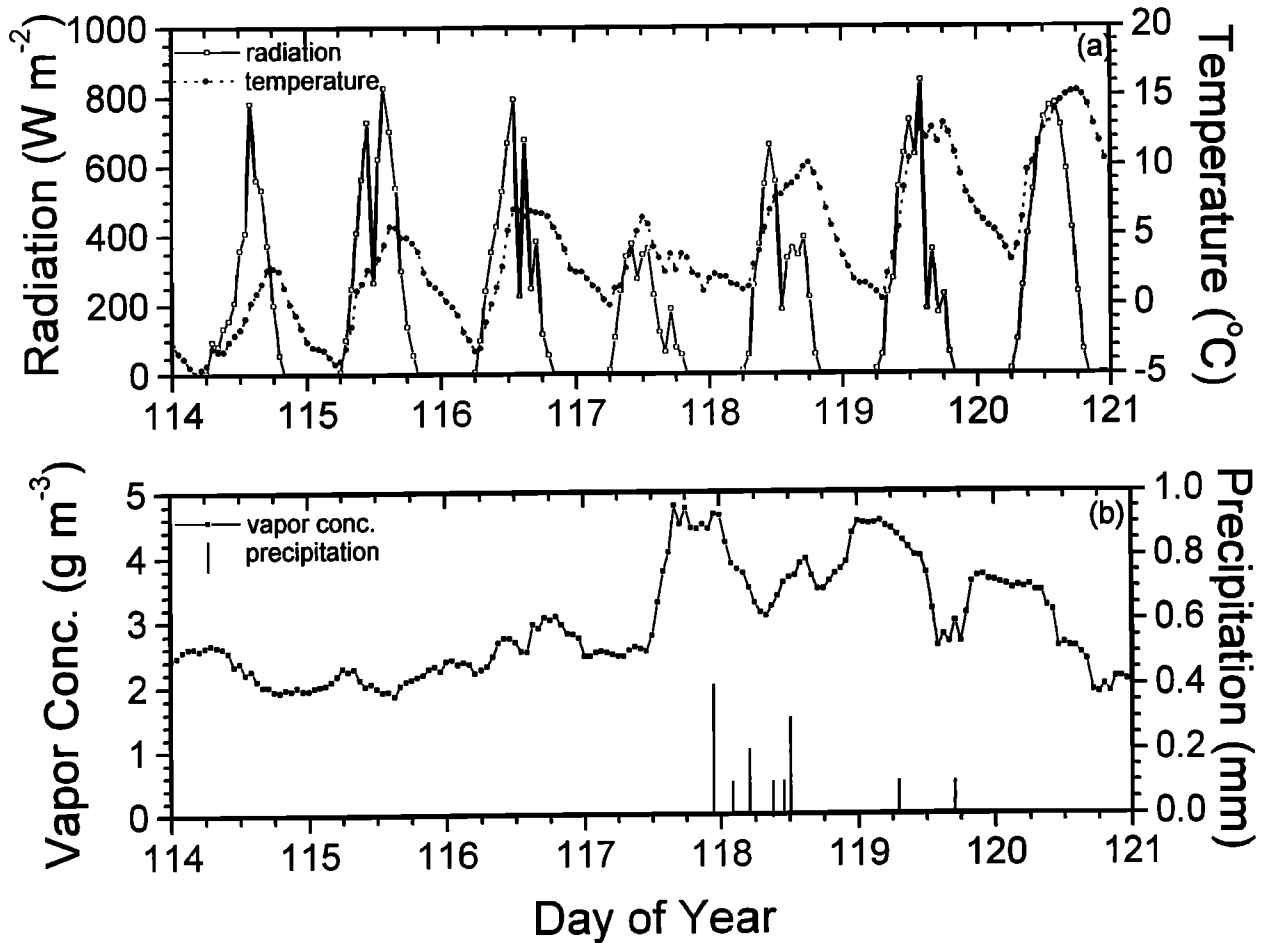


Figure 3. (a) Radiation, air temperature, (b) vapor concentration and precipitation during the April comparison period.

0.78, $b = 0.94 \pm 0.04$; over hazelnut, $R^2 = 0.63$, $b = 1.22 \pm 0.08$). In the model, large upward sensible heat fluxes were simulated from the recently dry forest litter layer. This layer warmed to temperatures several degrees above those of the air, and as much as 10°C above those of the soil surface underneath, because of its exposure to solar radiation, its low heat capacity, and its low thermal conductivity. Similarly large temperature differences were measured at the field site at this time of the year [Blanken *et al.*, 1997]. Differences in net radiation and sensible heat flux simulated over aspen and hazelnut were due to interception of irradiance by aspen stem surfaces (Figure 4a versus Figure 4b).

CO_2 fluxes during late April remained small (Figure 5) because soil respiration was constrained by low soil temperatures under the forest litter layer and because plant respiration and fixation were constrained by the absence of leaves. A respiration flux of about $2 \mu\text{mol m}^{-2} \text{s}^{-1}$ from the hazelnut canopy in the model was caused by remobilization of storage C before leaf-out. Small downward fluxes simulated late in the comparison period indicate the beginning of CO_2 fixation by emerging leaves, although leaf emergence in the field did not begin until a few days later.

5.2.2. Late spring. Air temperatures and vapor concentrations were higher during the second comparison period than during the first (average daytime RH $\approx 60\%$). During the last two days of this period the weather became cloudy, cool (Fig-

ure 6a), and rainy (Figure 6b). Data for net radiation were available only over the aspen for the first and last days of the period but were close to simulated values (Figure 7a). At this time, total canopy leaf area in the model was $6 \text{ m}^2 \text{ m}^{-2}$ about evenly divided between aspen and hazelnut, while that in the field was about $5 \text{ m}^2 \text{ m}^{-2}$, of which hazelnut was slightly larger than aspen. The recent completion of leaf-out caused net radiation and, consequently, mass and energy exchange to be much smaller over the hazelnut than over the aspen canopy (Figure 7b), indicating preferential interception of irradiance by the dominant aspen canopy. The ratio of net radiation simulated over hazelnut versus aspen in the model was partly affected by the interception fraction used for aspen (Table 3). This ratio increased with solar angle from 0.20 in the morning and evening to 0.25 at midday (Figure 7a versus Figure 7b) which was close to one of 0.26 calculated for mid-June from net radiation measurements at 4 versus 39 m [Chen *et al.*, 1997].

During this period, slightly more radiant energy was partitioned into latent heat than into sensible heat over both the aspen and the hazelnut canopies (Figure 7). In the model, energy partitioning was controlled by canopy conductance aggregated from leaf conductances which were determined by leaf CO_2 fixation rates and turgor potentials. Leaf CO_2 fixation rates were determined by irradiance and temperature at the leaf surfaces (Figure 2), and leaf turgor potential potentials

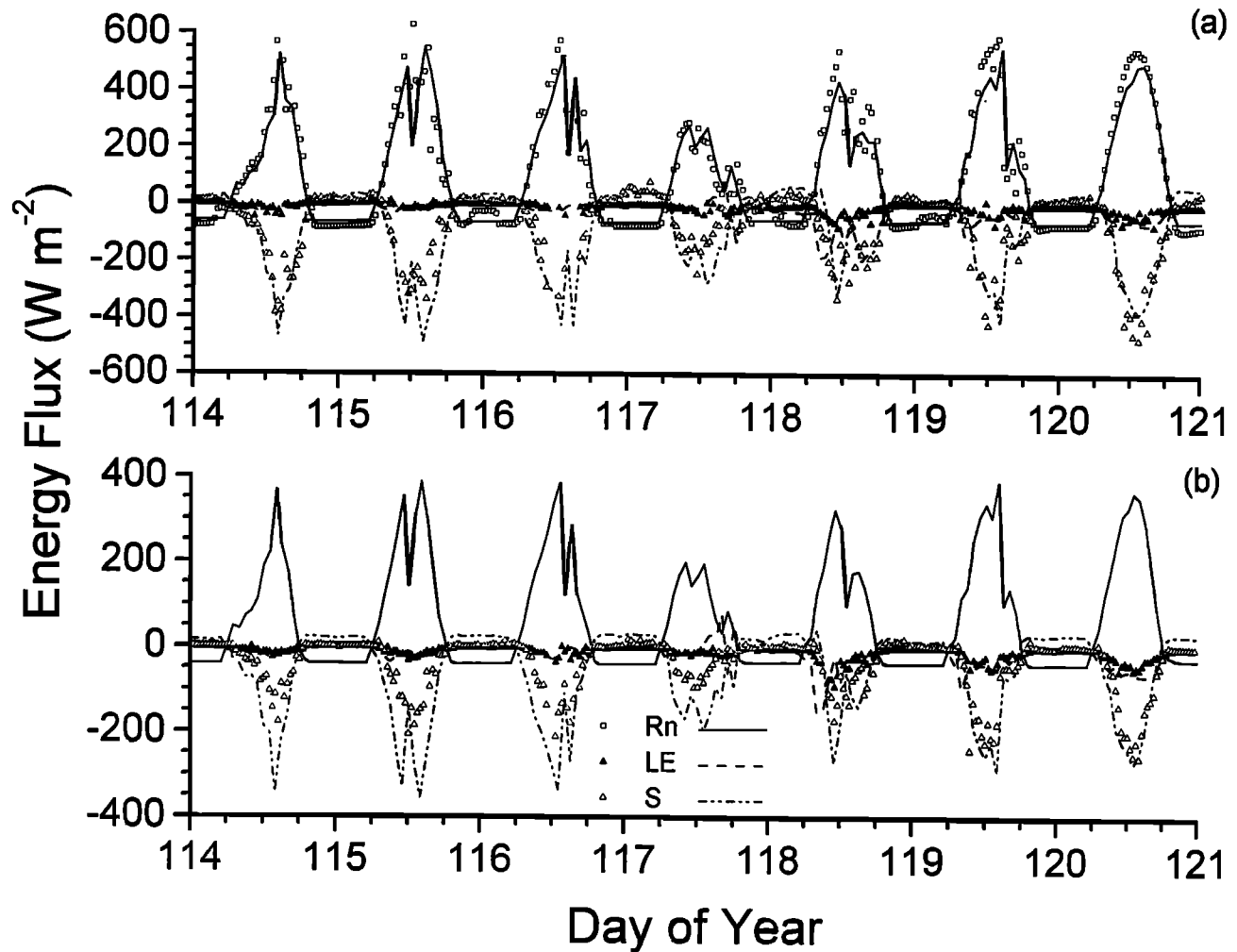


Figure 4. Energy fluxes simulated (lines) and measured (symbols) over (a) the aspen overstory and (b) the hazelnut understory during the April comparison period.

were determined by transpiration fluxes controlled by soil and atmospheric water status. Thus higher solar radiation and air temperatures during DOY 161 and 162 versus other DOY (Figure 6a) caused greater leaf CO_2 fixation (Figure 8), and hence greater leaf conductance, leading to greater upward latent heat fluxes (Figures 7a, 7b). Greater upward fluxes were also measured during these two days, so that model fluxes followed changes in diurnal trends of measured values during the week (simulated versus measured latent heat fluxes: over aspen, $R^2 = 0.79$, $b = 1.19 \pm 0.05$; over hazelnut, $R^2 = 0.56$, $b = 0.68 \pm 0.05$). Turgor potentials in the model remained high during this period, so stomatal conductance was little affected by soil and atmospheric water status. Cool rainy weather during DOY 164 and 165 caused measured and simulated fluxes to remain small.

CO_2 fluxes simulated and measured over the aspen during this period reached downward rates of $20\text{--}25 \mu\text{mol m}^{-2} \text{s}^{-1}$ during the days, indicating active fixation by aspen plus hazelnut leaves, and upward rates of $5\text{--}10 \mu\text{mol m}^{-2} \text{s}^{-1}$ during the nights, indicating aspen plus hazelnut plus soil respiration (Figure 8). In the model, overstory CO_2 fluxes were the net results of aggregated CO_2 fixation at leaf surfaces (responses to irradiance and temperature shown in Figure 2), of aggregated branch respiration by both aspen and hazelnut canopies, and of

aggregated root and microbial respiration (Table 3) through the soil profile. Downward fluxes simulated over the aspen were close to those measured under lower irradiance and cooler temperatures during DOY 159 and 160 but were greater than those measured under higher irradiance and warmer temperatures (Figure 6a) during DOY 161 and 162 because measured fluxes did not respond to improved weather on these dates (simulated versus measured CO_2 fluxes: over aspen, $R^2 = 0.80$, $b = 1.23 \pm 0.05$; over hazelnut, $R^2 = 0.24$, $b = 0.32 \pm 0.05$). Wind speeds remained below 1 m s^{-1} on DOY 159, 160, and 163, possibly causing some scatter in the measured values. Both measured and simulated downward CO_2 fluxes were reduced by lower radiation and cooler temperatures during the last two days of the comparison period. Fluxes measured and simulated over the hazelnut varied from downward rates of less than $5 \mu\text{mol m}^{-2} \text{s}^{-1}$ during the days, reduced by shading from the aspen overstory, to upward rates of $5\text{--}10 \mu\text{mol m}^{-2} \text{s}^{-1}$ during the nights, indicating that hazelnut net CO_2 fixation was slightly less than soil plus aboveground hazelnut respiration. Greater upward CO_2 fluxes measured and simulated during the nights over aspen versus hazelnut indicate aspen canopy respiration above 4 m.

5.2.3. Midsummer. There was one cool, cloudy day in the middle of the midsummer comparison period (DOY 199),

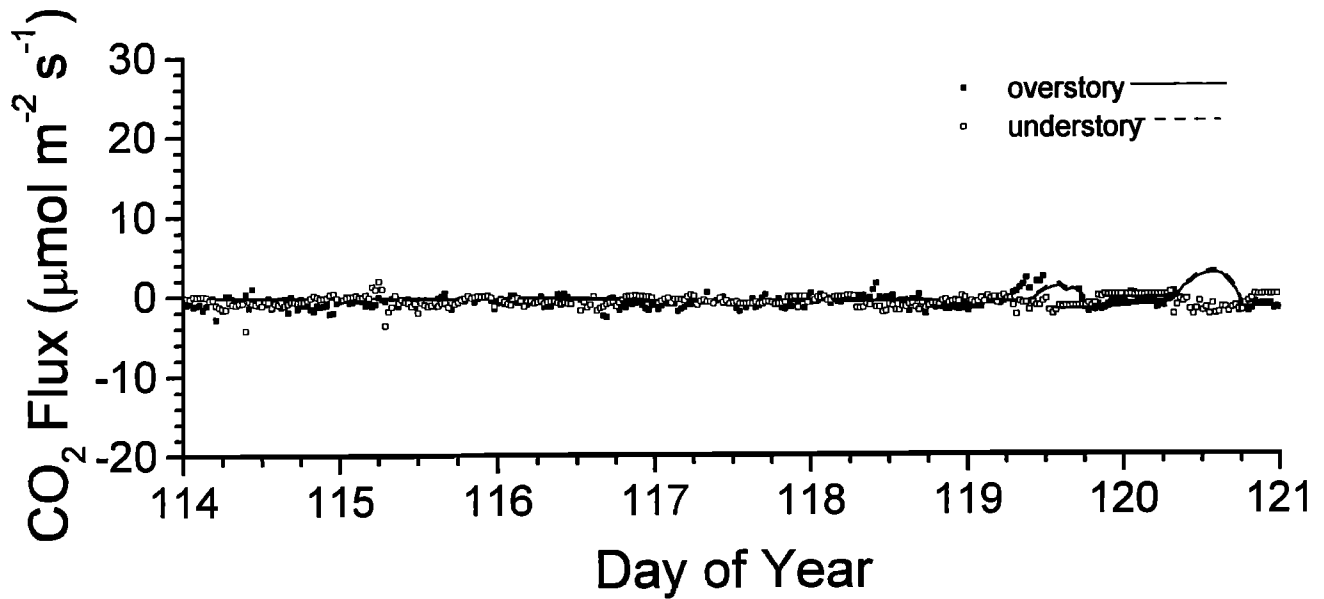


Figure 5. CO₂ fluxes simulated (lines) and measured (symbols) over the aspen overstory and the hazelnut understory during the April comparison period.

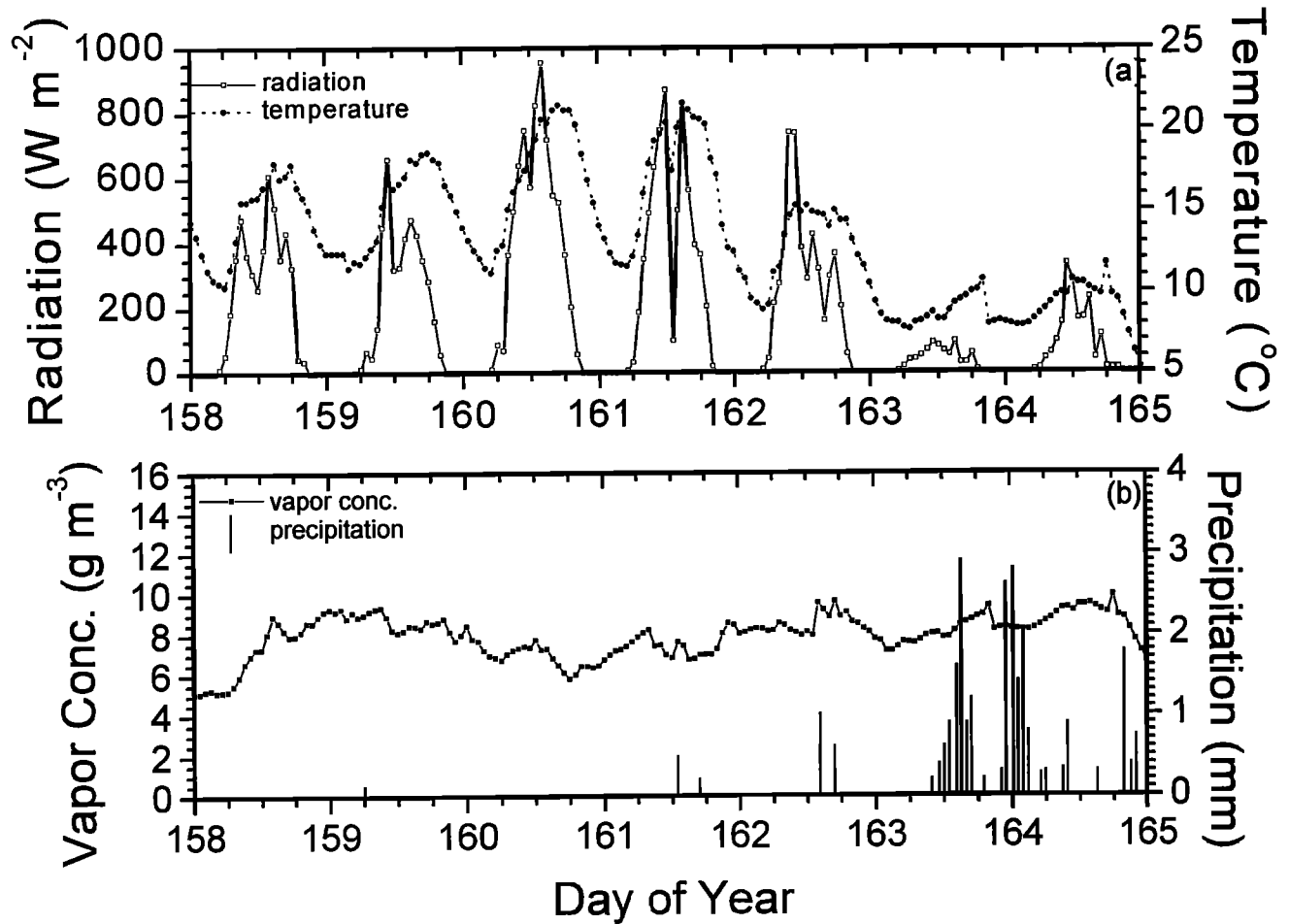


Figure 6. (a) Radiation, air temperature, (b) vapor concentration and precipitation during the June comparison period.

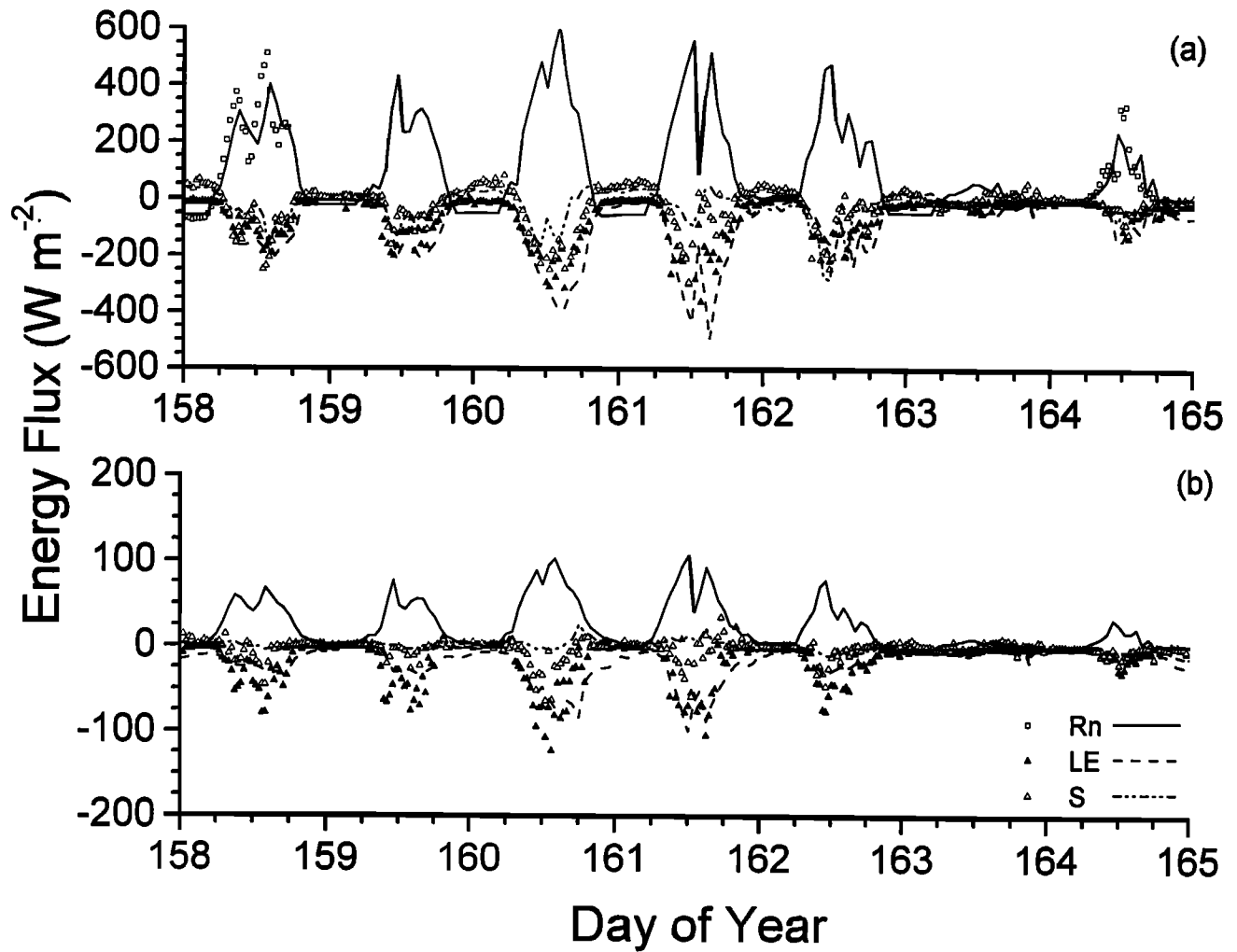


Figure 7. Energy fluxes simulated (lines) and measured (symbols) over (a) the aspen overstory and (b) the hazelnut understory during the June comparison period.

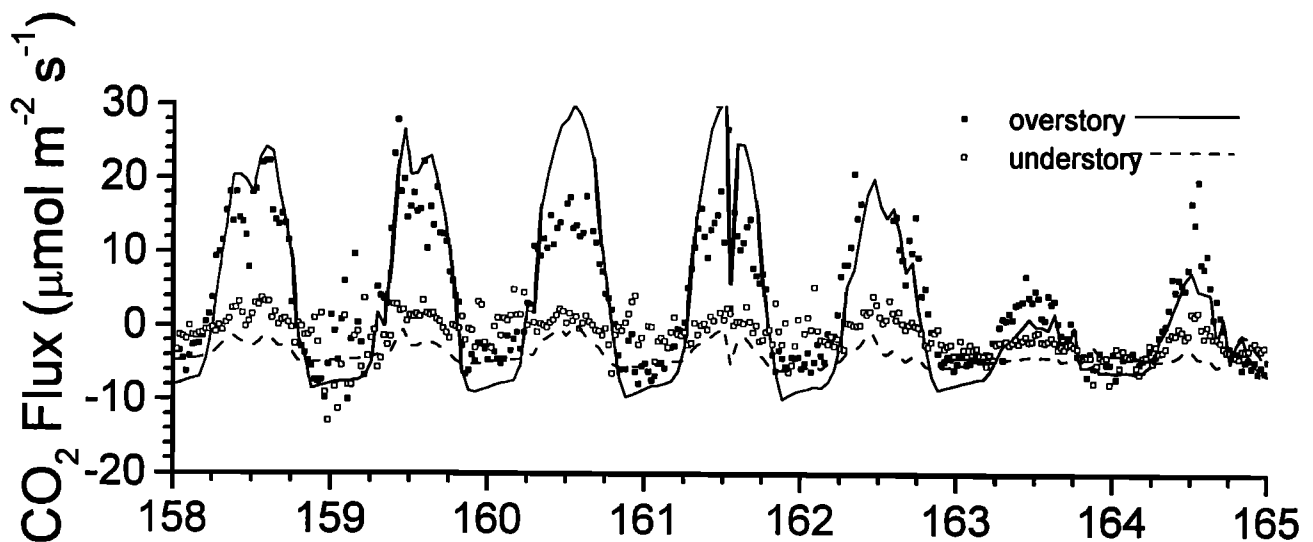


Figure 8. CO_2 fluxes simulated (lines) and measured (symbols) over the aspen overstory and the hazelnut understory during the June comparison period.

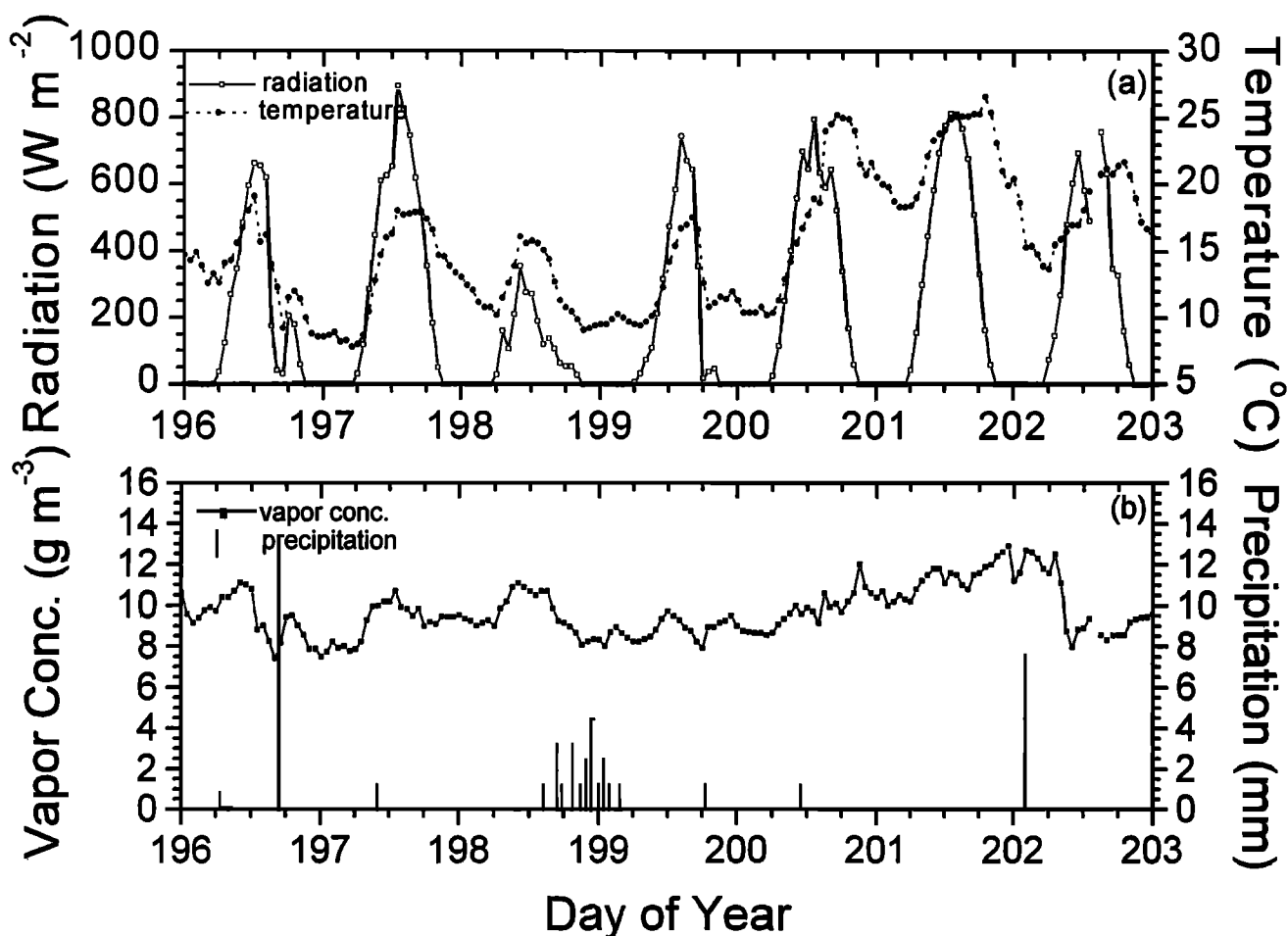


Figure 9. (a) Radiation, air temperature, (b) vapor concentration and precipitation during the July comparison period.

followed by warm, clear weather (Figure 9a) with stable vapor concentration (average daytime RH \approx 55%) (Figure 9b). Total canopy leaf area and its distribution between aspen and hazelnut was similar to that in late spring both in the model and at the field site. The ratio of net radiation simulated over hazelnut versus aspen (Figure 10b versus Figure 10a) followed the same diurnal range of 0.20–0.25 as that during late spring, while the ratio measured at 4 versus 39 m declined from 0.26 to 0.23. Most radiant energy received by both the aspen and the hazelnut canopies at this time was returned to the atmosphere as latent heat, fluxes of which reached 400 W m^{-2} during the warm weather that followed rainfall on DOY 199 (Figure 10a). Sensible heat fluxes remained low, especially over the hazelnut (Figure 10b). In the model, high radiation and air temperatures following rainfall on DOY 199 (Figure 9a) caused rapid leaf CO_2 fixation (e.g., Figure 2), and hence large leaf and canopy conductances. These conductances, combined with relatively high canopy-atmosphere vapor pressure differences generated by higher canopy temperatures and moderate vapor concentrations (Figure 9b), caused most radiant energy to be partitioned to latent heat flux later in the comparison period (Figures 10a, 10b). Measured latent heat fluxes were also large at this time (simulated versus measured latent heat fluxes during the week: over aspen, $R^2 = 0.78$, $b = 0.97 \pm 0.04$; over hazelnut, $R^2 = 0.72$, $b = 0.99 \pm 0.05$). Canopy turgor in the model remained high during this

period, so canopy conductances were little affected by soil and atmospheric water status.

Diurnal trends in CO_2 fluxes measured and simulated during this period (Figure 11) were similar to those during the late spring (Figure 8), with smaller downward and upward rates occurring under cool, cloudy weather on DOY 199 (Figure 9a) and greater downward and upward rates under warm, clear weather afterward. These fluxes are driven by the aggregated responses of leaf CO_2 fixation to irradiance and temperature, as shown in Figure 2. As during the late spring comparison period (Figure 8), fluxes simulated under higher irradiance and warmer temperatures (after DOY 200) were higher than those measured, while those simulated under lower irradiance and cooler temperatures (DOY 197, 200) were closer (simulated versus measured CO_2 fluxes during the week: over aspen, $R^2 = 0.74$, $b = 0.94 \pm 0.04$; over hazelnut, $R^2 = 0.04$, $b = 0.17 \pm 0.06$). Wind speeds remained near or below 1 m s^{-1} before DOY 200, possibly causing some scatter in the measured values. Fluxes measured and simulated over the hazelnut varied from downward rates of less than $5 \mu\text{mol m}^{-2} \text{ s}^{-1}$ during the days to upward rates of $10 \mu\text{mol m}^{-2} \text{ s}^{-1}$ during the nights, indicating that hazelnut net CO_2 fixation was less than soil plus aboveground hazelnut respiration. More rapid upward CO_2 fluxes simulated during midsummer versus late spring were caused by the effects of higher temperatures on growth and maintenance respiration of plant and microbial

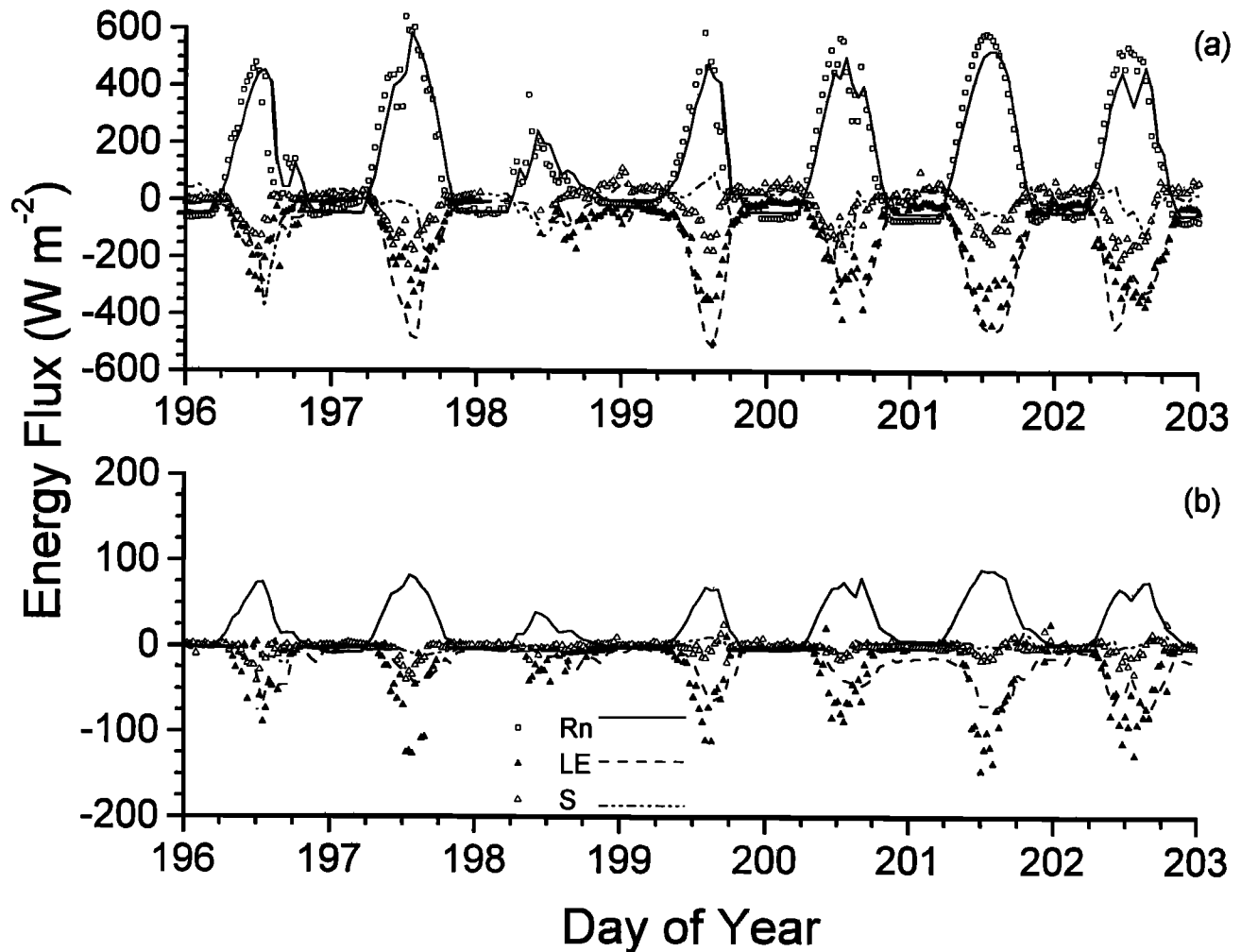


Figure 10. Energy fluxes simulated (lines) and measured (symbols) over (a) the aspen overstory and (b) the hazelnut understory during the July comparison period.

populations. Fluxes simulated over hazelnut were about $2 \mu\text{mol m}^{-2} \text{s}^{-1}$ more upward than those measured because soil respiration in the model was greater than that measured during this period (Figure 12).

5.3. Annual Carbon and Water Exchange

Annual C exchange accumulated from hourly values in the model is compared with that estimated from measured C fluxes according to *Black et al.* [1996] and from allometric techniques according to *Gower et al.* [1997] (Table 4). Annual ecosystem gross CO_2 fixation of 1132 g C m^{-2} in the model was 11% greater than that estimated by *Black et al.* [1996]. Fixation by aspen in the model was more than that estimated (811 versus 690 g C m^{-2}), while fixation by hazelnut in the model was similar to that estimated (321 versus 330 g C m^{-2}). The partitioning of CO_2 fixation in the model was due to canopy dominance effects on the interception of photosynthetic irradiance that caused higher irradiance intensities at leaf surfaces and consequently higher rates of leaf CO_2 fixation (Figure 2) by the taller aspen canopy (Figures 8 and 11).

Annual ecosystem respiration of 1064 g C m^{-2} in the model was 20% greater than that estimated by *Black et al.* [1996] (Table 4). Gross fixation and respiration estimated from aggregated fluxes measured above the aspen canopy may have

been reduced by refixation of respired CO_2 within the canopy, although the extent to which this occurred could not be evaluated. Respiration in the model was partitioned more to the aboveground aspen (271 g C m^{-2}) and less to the soil plus aboveground hazelnut (793 g C m^{-2}) than was the estimated respiration (20 and 870 g C m^{-2}). Annual aboveground respiration of aspen and hazelnut in the model is the sum of growth and maintenance requirements for all leaves, twigs, branches, stems, and reproductive biomass in each canopy. Aspen leaf biomass in the model reached a maximum value of 100 g C m^{-2} during the year of study, which was close to the average value of 90 g C m^{-2} measured at several sites in the field. This biomass would require about 50 g C m^{-2} for growth respiration and at least $75 \text{ g C m}^{-2} \text{ yr}^{-1}$ for maintenance respiration using published respiration coefficients. Aspen sapwood biomass after 80 years of the model run was 7.9 kg C m^{-2} , which was the same as that measured at the site. Annual requirements for growth and maintenance respiration of this biomass have been estimated by *Lavigne and Ryan* [1997] to be about 60 g C m^{-2} and $80 \text{ g C m}^{-2} \text{ yr}^{-1}$, respectively. Additional requirements for growth and maintenance of twigs and reproductive biomass also contributed to the model total of 271 g C m^{-2} for aboveground aspen respiration (Table 4). A corre-

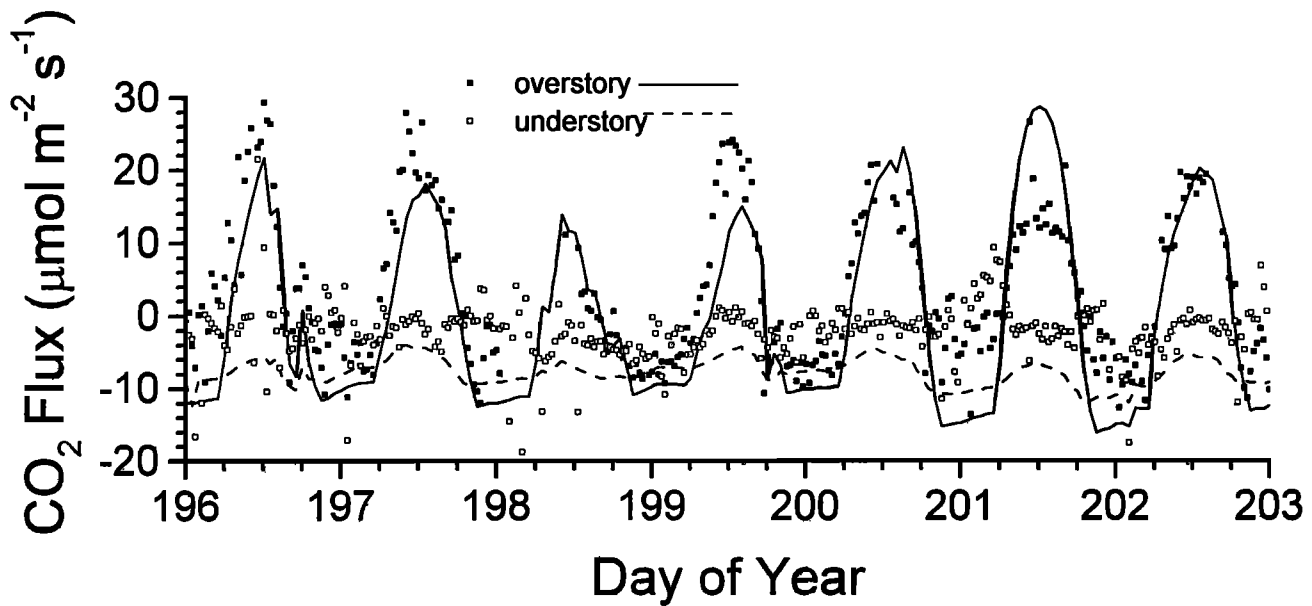


Figure 11. CO_2 fluxes simulated (lines) and measured (symbols) over the aspen overstory and the hazelnut understory during the July comparison period.

sponding total of 115 g C m^{-2} for aboveground hazelnut respiration, plus 525 g C m^{-2} soil respiration and 154 g C m^{-2} aspen plus hazelnut root respiration caused the soil plus hazelnut to be a net source of 472 g C m^{-2} in the model. Soil plus root respiration followed a pronounced annual cycle in both the model and at the field site (Figure 12), rising to almost $10 \mu\text{mol m}^{-2} \text{ s}^{-1}$ by midyear and then declining. In the model the annual respiration cycle was driven by changes in soil temperature and water content and by changes in plant phenology that determined changes in the partitioning of plant C to roots. This cycle was about 30 days earlier than that measured at the field site, although total annual values of modeled versus measured respiration were similar. The combination of the soil plus hazelnut source of 472 g C m^{-2} with the aboveground aspen sink of 540 g C m^{-2} gave a NEE in the model of 68 g C m^{-2} . Aggregation of measured C fluxes indicated a larger soil plus hazelnut source of 540 g C m^{-2} combined with a larger aspen sink of 670 g C m^{-2} which gave an estimated NEE of 130 g C m^{-2} [Black *et al.*, 1996]. Kimball *et al.* [1997] simulated a NEE of 180 g C m^{-2} at this site during 1994 without explicitly accounting for the hazelnut understory.

Aboveground senescence of aspen and hazelnut in the

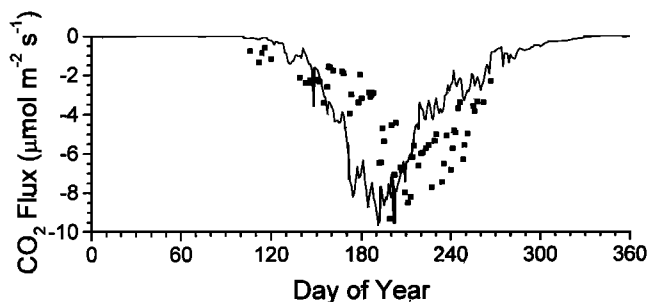


Figure 12. Soil CO_2 flux simulated (line) and measured (symbols) near midday during 1994 at the Southern Old Aspen site.

model included all biomass involved in the turnover of foliage, plus associated twigs and reproductive material. This senescence was greater than that measured from litter traps (216 versus 91 g C m^{-2} and 66 versus 32 g C m^{-2} from Table 4). Root senescence of aspen and hazelnut in the model included all biomass involved in the turnover of roots. This senescence of $57 + 24 = 81 \text{ g C m}^{-2}$ (Table 4) was similar to that of 46 g C m^{-2} estimated from root growth measured in growth cores and a fine root turnover index of between 1.5 and 2 calculated from minirhizotron measurements [Steele *et al.*, 1997]. Annual change in both aspen and hazelnut biomass in the model (112 and 41 g C m^{-2}) was about two-thirds that calculated from tree rings.

A greater fraction of annual evapotranspiration by the aspen-hazelnut forest was attributed to the soil in the model than in estimates from accumulated latent heat fluxes by Black *et al.* [1996] (Table 5). The partitioning of annual transpiration between aspen and hazelnut was similar in both model and field estimates. Partitioning in the model was determined by canopy dominance effects on irradiance interception and aerodynamic conductance. During the period of full leaf (June 15 to September 7), model versus field estimates of soil, hazelnut, and aspen contributions to total evapotranspiration were 0.12 versus 0.05, 0.16 versus 0.17, and 0.72 versus 0.78, respectively, indicating that most of the difference in the partitioning of evapotranspiration occurred when leaf area was low. Modeled and measured water use efficiencies of hazelnut (4.7 and $3.5 \text{ g C fixed kg}^{-1} \text{ water transpired}$) were higher than those of aspen (3.3 and $2.4 \text{ g C fixed kg}^{-1} \text{ water transpired}$), reflecting the lower irradiance to which the hazelnut was exposed.

5.4. Long-Term Net Ecosystem Exchange

Net ecosystem exchange varies with climate and with forest age. Annual values of NEE in the model (e.g., Table 4) were influenced by antecedent C storage in the aspen, hazelnut, and forest floor and by annual weather patterns through their different effects on C fixation and respiration. More definitive estimates of annual NEE in this forest should therefore be

Table 4. Annual Carbon Balance of a 70 Year Old Aspen-Hazelnut Forest Simulated by Ecosys and Estimated by Aggregating Short-Term Flux Measurements and by Measuring Changes in C Storage

| | g C m ⁻² | | |
|-------------------------------|---------------------|-----------------------|--------------------------|
| | Simulated by Ecosys | Estimated From Fluxes | Estimated From C Storage |
| <i>Aspen</i> | | | |
| Gross fixation | 811 | 690 | |
| Aboveground respiration | 271 | 20 | |
| Aboveground senescence | 216 | | 91 ^a |
| Aboveground net exchange | 540 | 670 | |
| Root respiration ^b | 109 | | |
| Root senescence | 57 | | |
| Root exudation | 102 | | |
| Change in biomass | 112 | | 173 |
| Change in storage | -56 | | |
| <i>Hazelnut</i> | | | |
| Gross fixation | 321 | 330 | |
| Aboveground respiration | 115 | | |
| Aboveground senescence | 66 | | 32 |
| Aboveground net exchange | 206 | | |
| Root respiration ^b | 45 | | |
| Root senescence | 24 | | |
| Root exudation | 34 | | |
| Change in biomass | 41 | | 66 |
| Change in storage | -4 | | |
| <i>Soil Plus Hazelnut</i> | | | |
| Soil respiration | 525 | | |
| Total respiration | 793 | 870 | |
| Net exchange | -472 | -540 | |
| <i>Ecosystem</i> | | | |
| Gross fixation | 1132 | 1020 | |
| Total respiration | 1064 | 890 | |
| <i>Net Ecosystem Exchange</i> | | | |
| | 68 | 130 | |

^aNonfoliar litter was distributed between aspen and hazelnut sources in proportion to their foliar litter.

^bRoot respiration includes only C oxidized for root maintenance and growth. C oxidized in the rhizosphere from root exudates and senesced root material is included in soil respiration.

derived from values simulated over several years. Average NEE simulated during years with warmer 1994 climate data (Table 6) were lower and more variable (i.e., more dependent upon antecedent C storage) than those during years with cooler 1995 or 1996 climate data because plant C fixation was raised by temperature comparatively less than were plant and soil C respiration (Table 6). I. A. Nalder and R. W. Wein (unpublished data, 1998) measured larger accumulations of forest floor C in similarly aged aspen stands under cooler

Table 5. Annual Evapotranspiration of an Aspen-Hazelnut Forest Simulated by Ecosys and Estimated by Aggregating Short-Term Flux Measurements

| | Simulated, mm | Estimated, mm |
|----------|---------------|---------------|
| Aspen | 245 | 284 |
| Hazelnut | 68 | 95 |
| Soil | 122 | 22 |
| Total | 435 | 401 |

versus warmer climates in the BOREAS study area. They suggested that C accumulation was more influenced by climate effects on forest floor decomposition than by those on plant growth.

The average rate of C accumulation in aspen wood from planting to 100 years of age in the model was 96 g C m⁻² yr⁻¹. This rate is similar to a rate of 80 g C m⁻² yr⁻¹ calculated at productive sites in the aspen parkland of central Saskatchewan derived from measurements of wood volume [Kirby *et al.*, 1957] and bulk density [Campbell *et al.*, 1985], and a rate of 98 g C m⁻² yr⁻¹ calculated from wood biomass of differently aged aspen stands in Prince Albert National Park near the Southern Old Aspen site (Figure 13). Carbon in the model also accumulated in the forest floor and the mineral soil below. Part of the accumulation in the forest floor appeared as surface residue, values of which stabilized at about 1.8 kg C m⁻² after 40 years of the model run. Halliwell *et al.* [1995] reported accumulations of surface detritus >5 mm diameter of about 1 kg C m⁻² using a line intersect method under mature aspen stands in Saskatchewan. The simulated accumulation of C in the wood and soil was sustained by an average N₂ fixation rate of 2.5 g N m⁻² yr⁻¹ in the model which is within the range of 0.35 to 3.25 g N m⁻² yr⁻¹ measured in soil of aspen stands by Brouzes *et al.* [1969].

6. Discussion

Complex ecosystem models such as ecosys are intended to function at levels of temporal and spatial resolution which extend from the higher levels at which individual processes (e.g., leaf C fixation, microbial C oxidation) occur to the lower levels at which changes in ecosystem behavior (e.g., NPP, NEE) occur. The sensitivity of individual processes in such models to defined changes in boundary conditions can be tested directly against experimental results at high temporal (hours) and spatial (cm²) resolution (e.g., leaf C fixation in Figure 2; microbial C oxidation [Grant and Rochette, 1994]). Such tests are well constrained because test results arise from a single process (e.g., leaf C fixation) with unique responses to independently controlled changes in boundary conditions (e.g., irradiance, temperature, CO₂). Testing at this level of resolution is of great importance in supporting model estimates of changes in NEE caused by changes in atmospheric CO₂ and temperature. The results of these tests may be used to support tests in which the sensitivity of spatially aggregated processes to uncontrolled changes in boundary conditions are tested against experimental results at comparable temporal (hours) and lower spatial (m²) resolution (e.g., Figures 4 to 11). Such

Table 6. Average Net Primary Productivity (NPP) and Net Ecosystem Exchange (NEE) Simulated (\pm Standard Deviation of Interannual Variability) in a Mixed Aspen-Hazelnut Forest Between 65 and 80 Years of Age During Years With 1994, 1995, and 1996 Climate Data

| | Climate Data, g C m ⁻² y ⁻¹ | | | |
|------|---|--------------|------------------|--------------|
| | NPP Aspen | NPP Hazel | Soil Respiration | NEE |
| 1994 | 446 \pm 24 | 174 \pm 17 | 514 \pm 57 | 105 \pm 84 |
| 1995 | 376 \pm 32 | 200 \pm 52 | 316 \pm 22 | 260 \pm 17 |
| 1996 | 352 \pm 28 | 170 \pm 30 | 362 \pm 12 | 161 \pm 24 |

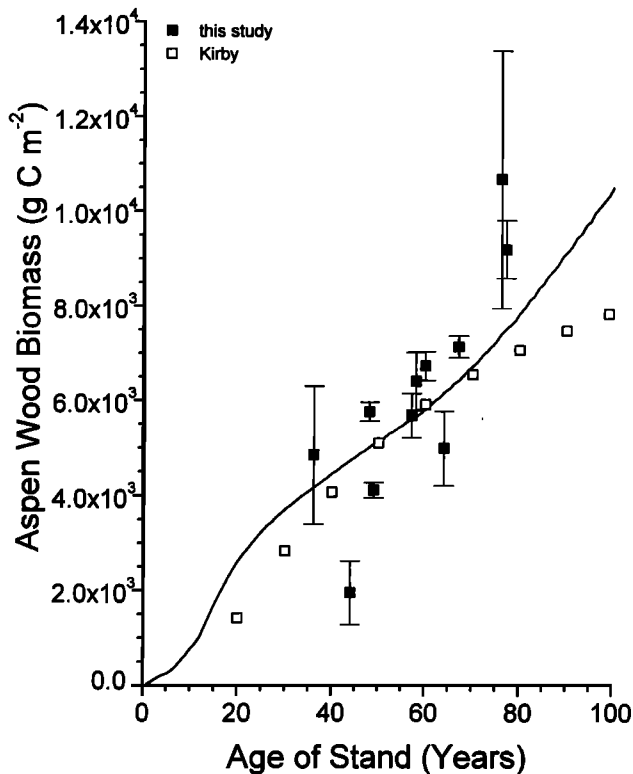


Figure 13. Growth of aspen wood simulated (line) and derived from species-specific allometric equations by Kirby [1957] in central Saskatchewan, and by Nalder (this article) in Prince Albert National Park, Saskatchewan.

tests are less well constrained than those conducted at higher resolution because test data are the net product of several interacting processes (e.g., leaf C fixation versus plant and microbial respiration), each of which responds differently to changes in boundary conditions. These tests are also less well constrained because changes in individual boundary conditions are correlated rather than independent (e.g., diurnal changes in temperature follow those of irradiance). These tests are therefore less able to discriminate among alternative model hypotheses (e.g., the accuracy of alternative hypotheses for sensitivity to irradiance versus temperature may not be distinguished). The results of these tests may in turn be used to support tests in which the sensitivity of temporally aggregated processes (e.g., NEE) to uncontrolled changes in boundary conditions are tested against experimental results at comparable spatial (m^2) and lower temporal (years) resolution (e.g., Figures 12 and 13, Tables 4–6). Such tests are of greatest ecological interest but are very poorly constrained because the test data is of low precision and may be explained by a wide range of alternative model hypotheses, not all of which may be widely applicable. It is therefore imperative that such tests be extensively supported by better constrained tests conducted at higher levels of temporal and spatial resolution before ecosystem models are used for predictive purposes. The need for such tests has driven the development of more complex models such as *ecosys*.

Diurnal changes in leaf C fixation simulated under diurnal changes in irradiance, temperature, humidity and wind speed, when aggregated to the canopy level and combined with aggregated organ respiration, explained between 70 and 80% of

diurnal variation in CO_2 exchange measured over the aspen canopy (Figures 8 and 11). Diurnal changes in leaf fixation drove those in leaf conductance which, when aggregated to the canopy level and used in a first-order solution to the canopy energy balance, explained between 70% and 80% of diurnal variation in latent heat flux measured over the aspen canopy (Figures 7 and 10). Except for a tendency to overestimate downward CO_2 flux in late spring, there were no apparent biases in the modeled fluxes (b values not significantly different from 1). Without an independent estimate of scatter in the measured fluxes, there is no objective method to establish the extent of agreement between simulated and measured values. However, evidence presented in Figures 6–11 suggests that the aggregation techniques used in *ecosys* allow leaf-level behavior (Figure 2) to be represented at the canopy level. Such representation is important if canopy-level responses to changes in atmospheric temperature and CO_2 concentration are to be modeled accurately. Some improvement in model accuracy might be achieved by extending the resolution of temperature, humidity, and CO_2 concentration from the canopy to the leaf as is currently done for irradiance, but such improvement may be limited [Sinclair *et al.*, 1976]. Furthermore, the coupling of a spatially resolved canopy to the spatially resolved soil profile in *ecosys* would entail a considerable computational cost.

Algorithms in *ecosys* for the partitioning, accumulation and senescence of C, N, and P in different organs of each plant species (leaves, twigs, reproductive material, branches, main stems, primary, and secondary roots) allow diurnal changes in canopy mass and energy exchange to be aggregated from hourly to yearly and decadal timescales. The results from such aggregation can be tested against changes in plant and soil C measured over the same timescales (Tables 4–6, Figure 13). Such long-term tests can identify systematic biases in short-term model behavior that may require several years to become apparent in a model run, thereby providing important feedback to model development. Although these tests are of greatest relevance to the ecological questions being addressed by the model (e.g., longterm changes in NEE), they are very poorly constrained and have little scientific value except to support model testing at higher temporal and spatial resolution.

Model results at yearly and decadal timescales suggest that average NEE for a 50–80 year old aspen-hazelnut forest in the BOREAS southern study area is 160 to 170 $\text{g C m}^{-2} \text{yr}^{-1}$ (Table 6). This value may be larger for a younger forest in which the forest floor is still developing and may be smaller for an older forest in which NPP is declining. Because NEE is the difference between two much larger C exchanges, fixation and respiration (Table 4), comparatively small changes in either may cause comparatively large changes in NEE. Changes in fixation and respiration may cause NEE to become smaller during warmer years and larger during cooler years (Table 6), although changes in NEE will be affected by intra-annual trends in temperature and precipitation [Frolking, 1997]. It is therefore important that model estimates of changes in NEE continue to be tested against experimental estimates made over several years of contrasting weather. Such testing will support model estimates of long-term changes in NEE caused by changes in atmospheric CO_2 and temperature.

Acknowledgments. *Ecosys* was run on a SGI/CRAY Origin 2000 provided through the Multimedia Advanced Computational Infrastructure (MACI) project of the Universities of Alberta and Calgary.

References

- Allen, L. H., Jr., R. R. Valle, J. W. Mishoe, J. W. Jones, and P. H. Jones, Soybean leaf gas exchange responses to CO₂ enrichment, *Proc. Soil Crop Sci. Soc. Fla.*, **49**, 192–198, 1990.
- Ball, J. T., An analysis of stomatal conductance, 89 pp., Ph.D. thesis, Stanford Univ., Calif., 1988.
- Black, T. A., et al., Annual cycles of water vapour and carbon dioxide fluxes in and above a boreal aspen forest, *Global Change Biol.*, **2**, 219–229, 1996.
- Blanken, P. D., T. A. Black, P. C. Yang, H. H. Neumann, Z. Nestic, R. Staebler, G. den Hartog, M. D. Novak, and X. Lee, Energy balance and canopy conductance of a boreal aspen forest: Partitioning overstory and understory components, *J. Geophys. Res.*, **102**, 28,915–28,927, 1997.
- Bonan, G. B., K. J. Davis, D. Baldocchi, D. Fitzjarrald, and H. Neumann, Comparison of NCAR LSM1 land surface model with BOREAS aspen and jack pine tower fluxes, *J. Geophys. Res.*, **102**, 29,065–29,075, 1997.
- Brouzes, R., J. Lasik, and R. Knowles, The effect of organic amendment, water content and oxygen on the incorporation of ¹⁵N₂ by some agricultural and forest soils, *Can. J. Microbiol.*, **15**, 899–905, 1969.
- Campbell, J. S., V. J. Liefers, and E. C. Pielou, Regression equations for estimating single tree biomass of trembling aspen: Assessing their applicability to more than one population, *For. Ecol. Manage.*, **11**, 283–295, 1985.
- Chaudhuri, U. N., M. B. Kirkham, and E. T. Kanemasu, Carbon dioxide and water level effects on yield and water use of winter wheat, *Agron. J.*, **82**, 637–641, 1990.
- Chen, J. M., P. D. Blanken, T. A. Black, M. Guilbeault, and S. Chen, Radiation regime and canopy architecture in a boreal aspen forest, *Agric. For. Meteorol.*, **86**, 107–125, 1997.
- Choudhury, B. J., and J. L. Monteith, A four-layer model for the heat budget of homogenous land surfaces, *Q. J. R. Meteorol. Soc.*, **114**, 373–398, 1988.
- Cowan, I. R., Transport of water in the soil-plant-atmosphere system, *J. Appl. Ecol.*, **2**, 221–239, 1965.
- Curtis, P. S., A meta-analysis of leaf gas exchange and nitrogen in trees grown under elevated carbon dioxide, *Plant Cell Environ.*, **19**, 127–137, 1996.
- Dang, Q. L., H. A. Margolis, S. Y. Mikailou, M. R. Coyea, G. J. Collatz, and C. L. Walthall, Profiles of photosynthetically active radiation, nitrogen, and photosynthetic capacity in the boreal forest: Implications for scaling from leaf to canopy, *J. Geophys. Res.*, **102**, 28,845–28,860, 1997.
- Farquhar, G. D., S. von Caemmerer, and J. A. Berry, A biochemical model of photosynthetic CO₂ assimilation in leaves of C₃ species, *Planta*, **149**, 78–90, 1980.
- Frolking, S., Sensitivity of spruce/moss boreal forest net ecosystem productivity to seasonal anomalies in weather, *J. Geophys. Res.*, **102**, 29,053–29,064, 1997.
- Gollan, T., J. B. Passioura, and R. Munns, Soil water status affects the stomatal conductance of fully turgid wheat and sunflower leaves, *Aust. J. Plant Phys.*, **13**, 459–464, 1986.
- Gower, S. T., J. G. Vogel, T. K. Stow, J. M. Norman, C. J. Kucharik, and S. J. Steele, Carbon distribution and aboveground net-primary production in aspen, jack pine, and black spruce stands in Saskatchewan and Manitoba, Canada, *J. Geophys. Res.*, **102**, 29,029–29,042, 1997.
- Grant, R. F., Dynamic simulation of phase changes in snowpacks and soils, *Soil Sci. Soc. Am. J.*, **56**, 1051–1062, 1992.
- Grant, R. F., Simulation model of soil compaction and root growth, I, Model development, *Plant Soil*, **150**, 1–14, 1993a.
- Grant, R. F., Simulation model of soil compaction and root growth, II, Model testing, *Plant Soil*, **150**, 15–24, 1993b.
- Grant, R. F., Rhizodeposition by crop plants and its relationship to microbial activity and nitrogen distribution, *Mod. Geol. Biol. Proc.*, **2**, 193–209, 1993c.
- Grant, R. F., Simulation of competition between barley (*Hordeum vulgare* L.) and wild oat (*Avena fatua* L.) under different managements and climates, *Ecol. Model.*, **71**, 269–287, 1994a.
- Grant, R. F., Simulation of ecological controls on nitrification, *Soil Biol. Biochem.*, **26**, 305–315, 1994b.
- Grant, R. F., Mathematical modelling of nitrous oxide evolution during nitrification, *Soil Biol. Biochem.*, **27**, 1117–1125, 1995.
- Grant, R. F., Ecosys, in *Global Change and Terrestrial Ecosystems Focus 3 Wheat Network, Model and Experimental Metadata*, 2nd ed., pp. 65–74, GCTE Focus 3 Off., NERC Cent. for Ecol. and Hydrol., Wallingford, Oxon, England, 1996a.
- Grant, R. F., Ecosys, in *Global Change and Terrestrial Ecosystems Task 3.3.1 Soil Organic Matter Network (SOMNET): 1996 Model and Experimental Metadata*, pp. 19–24, GCTE Focus 3 Off., NERC Cent. for Ecol. and Hydrol., Wallingford, Oxon, England, 1996b.
- Grant, R. F., Changes in soil organic matter under different tillage and rotation: Mathematical modelling in *ecosys*, *Soil Sci. Soc. Am. J.*, **61**, 1159–1174, 1997.
- Grant, R. F., Simulation in *ecosys* of root growth response to contrasting soil water and nitrogen, *Ecol. Model.*, **107**, 237–264, 1998a.
- Grant, R. F., Simulation of methanogenesis in the mathematical model *ecosys*, *Soil Biol. Biochem.*, **30**, 883–896, 1998b.
- Grant, R. F., Simulation of methanotrophy in the mathematical model *ecosys*, *Soil Biol. Biochem.*, **31**, 287–297, 1999.
- Grant, R. F., and D. D. Baldocchi, Energy transfer over crop canopies: Simulation and experimental verification, *Agric. For. Meteorol.*, **61**, 129–149, 1992.
- Grant, R. F., and D. J. Heaney, Inorganic phosphorus transformation and transport in soils: Mathematical modelling *ecosys*, *Soil Sci. Soc. Am. J.*, **61**, 752–764, 1997.
- Grant, R. F., and J. D. Hesketh, Canopy structure of maize (*Zea mays* L.) at different populations: Simulation and experimental verification, *Biotronics*, **21**, 11–24, 1992.
- Grant, R. F., and E. Pattey, Mathematical modelling of nitrous oxide emissions from an agricultural field during spring thaw, *Global Biogeochem. Cycles*, in press, 1999.
- Grant, R. F., and J. A. Robertson, Phosphorus uptake by root systems: Mathematical modelling in *ecosys*, *Plant Soil*, **188**, 279–297, 1997.
- Grant, R. F., and P. Rochette, Soil microbial respiration at different temperatures and water potentials: Theory and mathematical modelling, *Soil Sci. Soc. Am. J.*, **58**, 1681–1690, 1994.
- Grant, R. F., N. G. Juma, and W. B. McGill, Simulation of carbon and nitrogen transformations in soils, I, Mineralization, *Soil Biol. Biochem.*, **27**, 1317–1329, 1993a.
- Grant, R. F., N. G. Juma, and W. B. McGill, Simulation of carbon and nitrogen transformations in soils, II, Microbial biomass and metabolic products, *Soil Biol. Biochem.*, **27**, 1331–1338, 1993b.
- Grant, R. F., M. Nyborg, and J. Laidlaw, Evolution of nitrous oxide from soil, I, Model development, *Soil Sci.*, **156**, 259–265, 1993c.
- Grant, R. F., M. Nyborg, and J. Laidlaw, Evolution of nitrous oxide from soil, II, Experimental results and model testing, *Soil Sci.*, **156**, 266–277, 1993d.
- Grant, R. F., P. Rochette, and R. L. Desjardins, Energy exchange and water use efficiency of crops in the field: Validation of a simulation model, *Agron. J.*, **85**, 916–928, 1993e.
- Grant, R. F., R. C. Izaurralde, and D. S. Chanasyk, Soil temperature under different surface managements: Testing a simulation model, *Agric. For. Meteorol.*, **73**, 89–113, 1995b.
- Grant, R. F., B. A. Kimball, P. J. Pinter Jr., G. W. Wall, R. L. Garcia, and R. L. LaMorte, CO₂ effects on crop energy balance: Testing *ecosys* with a Free-Air CO₂ Enrichment (FACE) experiment, *Agron. J.*, **87**, 446–457, 1995c.
- Grant, R. F., R. C. Izaurralde, M. Nyborg, S. S. Malhi, E. D. Solberg, and D. Jans-Hammermeister, Modelling tillage and surface residue effects on soil C storage under current vs. elevated CO₂ and temperature in *ecosys*, in *Soil Processes and the Carbon Cycle*, edited by R. Lal, J. M. Kimble, R. F. Follet, and B. A. Stewart, pp. 527–547, CRC Press, Boca Raton, Fla., 1997.
- Grant, R. F., G. W. Wall, K. F. A. Frumau, P. J. Pinter Jr., D. Hunsaker, B. A. Kimball, and R. L. LaMorte, Crop water relations under different CO₂ and irrigation: Testing of *ecosys* with the Free Air CO₂ Enrichment (FACE) experiment, *Agric. For. Meteorol.*, in press, 1998.
- Halliwell, D. H., M. J. Apps, and D. T. Price, A survey of the forest site characteristics in a transect through the central Canadian boreal forest, *Water Air Soil Pollut.*, **82**, 257–270, 1995.
- Hogg, E. H., and P. A. Hurdle, Sap flow in trembling aspen: Implications for stomatal responses to vapor pressure deficit, *Tree Physiol.*, **17**, 501–509, 1997.
- Iso, S. B., B. A. Kimball, M. G. Anderson, and J. R. Mauney, Effects of atmospheric CO₂ enrichment on plant growth: The interactive effect of air temperature, *Agric. Ecosyst. Environ.*, **20**, 1–10, 1987.
- Itoh, S., and S. A. Barber, Phosphorus uptake by six plant species as related to root hairs, *Agron. J.*, **75**, 457–461, 1983.

- Jenkinson, D. S., D. E. Adams, and A. Wild, Model estimates of CO₂ emissions from soils in response to global warming, *Nature*, 351, 304–306, 1991.
- Jordan, D. B., and W. L. Ogren, The CO₂/O₂ specificity of ribulose 1,5-bisphosphate carboxylase/oxygenase, *Planta*, 161, 308–313, 1984.
- Keeling, C. D., S. C. Piper, and M. Heimann, Global and hemispheric CO₂ sinks deduced from changes in atmospheric O₂ concentration, *Nature*, 318, 218–221, 1996.
- Kimball, B. A., Ecology of crops in changing CO₂ concentration, *J. Agric. Meteorol.*, 48, 559–566, 1993.
- Kimball, J. S., P. E. Thornton, M. A. White, and S. W. Running, Simulating forest productivity and surface-atmosphere carbon exchange in the BOREAS study region, *Tree Physiol.*, 17, 589–599, 1997.
- Kirby, C. L., W. S. Bailey, and J. G. Gilmour, The growth and yield of aspen in Saskatchewan, *Tech. Bull. 3*, Dep. of Nat. Resour., Saskatchewan, 1957.
- Kirschbaum, M. U. F., The temperature dependence of soil organic matter decomposition and the effect of global warming on soil organic C storage, *Soil Biol. Biochem.*, 27, 753–760, 1995.
- Lavigne, M. B., and M. G. Ryan, Growth and maintenance respiration rates of aspen, black spruce and jack pine stems at northern and southern BOREAS sites, *Tree Physiol.*, 17, 543–551, 1997.
- Margolis, H. A., and M. G. Ryan, A physiological basis for biosphere-atmosphere interactions in the boreal forest: An overview, *Tree Physiol.*, 17, 491–499, 1997.
- Parton, W. J., J. M. O. Scurlock, D. S. Ojima, D. S. Schimel, D. O. Hall, and SCOPEGRAM group members, Impact of climate change on grassland production and soil carbon worldwide, *Global Change Biol.*, 1, 13–22, 1995.
- Perrier, A., Land surface processes: Vegetation, in *Atmospheric General Circulation Models*, edited by P. S. Eagleson, pp. 395–448, Cambridge Univ. Press, New York, 1982.
- Reid, J. B., and M. G. Huck, Diurnal variation of crop hydraulic resistance: A new analysis, *Agron. J.*, 82, 827–834, 1990.
- Rogers, H. H., J. D. Cure, and J. M. Smith, Soybean growth and yield response to elevated carbon dioxide, *Agric. Ecosyst. Environ.*, 16, 113–128, 1986.
- Sellers, P. J., et al., A comparison of radiative and physiological effects of doubled CO₂ on the global climate, *Science*, 271, 1402–1406, 1996.
- Shewchuk, S. R., Surface mesoscale meteorological system for BOREAS, in *Proceedings of the 22nd Conference on Agricultural and Forest Meteorology*, pp. 42–44, Am. Meteorol. Soc., Boston, Mass., 1996.
- Sinclair, T. R., C. E. Murphy, and K. R. Knoerr, Development and evaluation of simplified models for simulating canopy photosynthesis and transpiration, *J. Appl. Ecol.*, 13, 813–829, 1976.
- Steele, S. J., S. T. Gower, J. G. Vogel, and J. M. Norman, Root mass, net primary production and turnover in aspen, jack pine and black spruce forests in Saskatchewan and Manitoba, Canada, *Tree Physiol.*, 17, 577–587, 1997.
- Stitt, M., Rising CO₂ levels and their potential significance for carbon flow in photosynthetic cells, *Plant Cell Environ.*, 14, 741–762, 1991.
- Trofymow, J. A., C. M. Preston, and C. E. Prescott, Litter quality and its potential effect on decay rates of materials from Canadian forests, *Water Air Soil Pollut.*, 82, 215–226, 1995.
- R. F. Grant and I. A. Nalder, Department of Renewable Resources, University of Alberta, Edmonton, Alberta, Canada T6G 2E1 (robert.grant@ualberta.ca)
- T. A. Black, P. D. Blanken, and P. C. Yang, Department of Soil Science, University of British Columbia, Vancouver, BC, Canada.
- G. den Hartog and H. H. Neumann, Atmospheric Environment Service, Environment Canada, Downsview, Ontario, Canada.
- J. A. Berry, Department of Plant Biology, Carnegie Institution of Washington, Stanford, CA.
- C. Russell, Department of Land Resource Science, University of Guelph, Guelph, Ontario, Canada.

(Received August 4, 1998; revised November 30, 1998; accepted December 8, 1998.)